

# Influence of Particle Phase State on the Hygroscopic Behavior of Mixed Organic-Inorganic Aerosols

N. Hodas,<sup>1</sup> A. Zuend,<sup>2</sup> W. Mui,<sup>3</sup> R. C. Flagan,<sup>1,3</sup> J. H. Seinfeld<sup>1,3</sup>

[1] Division of Chemistry and Chemical Engineering, California Institute of Technology, 1200 E. California Blvd., Pasadena, CA, USA

[2] Department of Atmospheric and Oceanic Sciences, McGill University, Montreal, Quebec, Canada

[3] Division of Engineering and Applied Science, California Institute of Technology, Pasadena, CA, USA

Correspondence to: N. Hodas (nhodas@caltech.edu)

## Abstract

Recent work has demonstrated that organic and mixed organic-inorganic particles can exhibit multiple phase states depending on their chemical composition and on ambient conditions such as relative humidity (RH). To explore the extent to which water uptake varies with particle phase behavior, hygroscopic growth factors (HGFs) of nine laboratory-generated, organic and organic-inorganic aerosol systems with physical states ranging from well-mixed liquids, to phase-separated particles, to viscous liquids or semi-solids were measured with the Differential Aerosol Sizing and Hygroscopicity Spectrometer Probe at RH values ranging from 40 – 90%. Water-uptake measurements were accompanied by HGF and RH-dependent thermodynamic equilibrium calculations using the Aerosol Inorganic-Organic Mixtures Functional groups Activity Coefficients (AIOMFAC) model. In addition, AIOMFAC-predicted growth curves are compared to several simplified HGF modeling approaches: (1) representing particles as ideal, well-mixed liquids, (2) forcing a single phase, but accounting for non-ideal interactions through activity coefficient calculations, and (3) a Zdanovskii-Stokes-Robinson-like calculation in which

1 complete separation between the inorganic and organic components is assumed at all RH values,  
2 with water-uptake treated separately in each of the individual phases. We observed variability in  
3 the characteristics of measured hygroscopic growth curves across aerosol systems with differing  
4 phase behaviors, with growth curves approaching smoother, more continuous water uptake with  
5 decreasing prevalence of liquid-liquid phase separation and increasing oxygen:carbon ratios of  
6 the organic aerosol components. We also observed indirect evidence for the dehydration-induced  
7 formation of highly viscous semi-solid phases and for kinetic limitations to the crystallization of  
8 ammonium sulfate at low RH for sucrose-containing particles. AIOMFAC-predicted growth  
9 curves are generally in good agreement with the HGF measurements. The performances of the  
10 simplified modeling approaches, however, differ for particles with differing phase states. This  
11 suggests that no single simplified modeling approach can be used to capture the water-uptake  
12 behavior for the diversity of particle phase behavior expected in the atmosphere. Errors in HGFs  
13 calculated with the simplified models are of sufficient magnitude to produce substantial error in  
14 estimates of particle optical and radiative properties, particularly for the assumption that water  
15 uptake is driven by absorptive equilibrium partitioning with ideal particle-phase mixing.

16

## 17 **1 Introduction**

18

19 Atmospheric aerosols alter the Earth's radiation budget, reduce visibility, and are  
20 associated with adverse health effects (Finlayson-Pitts and Pitts, 2000; Pöschl, 2005; Seinfeld  
21 and Pandis, 2006). The magnitude of these impacts is influenced by aerosol water content, as this  
22 is a major determinant of aerosol particle size. Further, aerosol water can impact gas-phase  
23 photochemistry and secondary organic aerosol (SOA) concentrations by serving as a sink for  
24 reactive gases and as a medium for aqueous-phase and heterogeneous reactions (Ervens et al.,  
25 2011, 2013). As a result, clear understanding of the hygroscopicity of atmospheric aerosols is  
26 key to representing aerosol properties and behavior in atmospheric models and to improving our  
27 understanding of their impacts on climate and air quality.

28 Organic aerosol (OA) comprises a substantial fraction of total aerosol mass (20 - 90%;  
29 Seinfeld and Pandis, 2006). Moreover, particle formation and transformation processes  
30 commonly lead to the formation of internally mixed organic-inorganic particles (Seinfeld and  
31 Pankow, 2003; Marcolli et al., 2004; Zhang et al., 2005; Murphy et al., 2006; Goldstein and

1 Galbally, 2007; Hallquist et al., 2009). Multiple studies have sought to elucidate the hygroscopic  
2 properties of OA, as well as the influence of organic aerosol components on the hygroscopic  
3 behavior and phase transitions of inorganic salts. Much of this work has focused on single- and  
4 multi-component aerosols comprised of carboxylic, dicarboxylic, and humic acids (e.g., Prenni et  
5 al., 2001; Choi and Chan, 2002a; Brooks et al., 2004; Chan et al., 2006; Moore and Raymond,  
6 2008; Hatch et al., 2009; Pope et al., 2010; Lei et al., 2014), as well as mixtures of organic acids  
7 with inorganic salts (e.g., Cruz and Pandis, 2000; Choi and Chan, 2002b; Prenni et al., 2003;  
8 Wise et al., 2003; Brooks et al., 2004; Svenningsson et al., 2006; Sjogren et al., 2007; Gao et al.,  
9 2008). Recent studies have explored water uptake by sugars, higher molecular weight organics,  
10 and polymers (Gysel et al., 2004; Mochida and Kawamura, 2004; Tong et al., 2011; Zobrist et  
11 al., 2011; Lei et al., 2014; Xu et al., 2014). Such studies have aimed to characterize the  
12 hygroscopicity of biomass burning aerosols, highly oxygenated, aged SOA, and oligomers. This  
13 body of research has demonstrated that the water-uptake behavior of OA components and their  
14 influence on the phase transitions of inorganics depend on multiple factors, including the  
15 composition and relative amounts of the organic and inorganic aerosol fractions, the  
16 physiochemical properties of the organic components, and ambient conditions. Controlled  
17 laboratory studies have also served as a basis for the development and evaluation of  
18 thermodynamic models (Clegg et al., 2001; Chan et al., 2005; Raatikainen and Laaksonen, 2005;  
19 Clegg and Seinfeld, 2006; Marcolli and Krieger, 2006; Svenningsson et al., 2006; Moore and  
20 Raymond, 2008; Zardini et al., 2008; Zuend et al., 2011; Lei et al., 2014), with the aim of  
21 representing water uptake by organic and mixed organic-inorganic aerosols.

22 Current regional and global chemical transport models include a simplified treatment of  
23 aerosol hygroscopicity. In CMAQ (Community Multi-scale Air Quality model), for example,  
24 only water uptake by the inorganic fraction is considered (Binkowski and Roselle, 2003;  
25 <http://www.epa.gov/AMD/Research/Air/aerosolModule.html>). In WRF-Chem (Weather  
26 Research and Forecasting model coupled with Chemistry), aerosol hygroscopicity depends on  
27 the aerosol module implemented. In MADE (Modal Aerosol Dynamics model for Europe) and  
28 MOSAIC (Model for Simulating Aerosol Interactions and Chemistry), only the inorganic aerosol  
29 components are considered in estimates of aerosol liquid water (Zaveri et al., 2008). In  
30 GOCART (Goddard Chemistry Aerosol Radiation and Transport), however, the influence of  
31 water uptake on the optical properties of OA is prescribed in tabulated, RH-dependent growth

1 factors (Koepke et al., 1997; <http://acmg.seas.harvard.edu/geos>). The Modal Aerosol Module  
2 (MAM) assumes the hygroscopicity of primary and secondary organic aerosol can each be  
3 described with a single parameter based on Köhler theory ( $\kappa$ ; Petters and Kreidenweis, 2007).  
4 Similarly, aerosol water associated with organic aerosol components is considered in GEOS-  
5 Chem (Goddard Earth Observing System coupled with chemistry) using a set of RH-dependent  
6 HGFs for total particulate organic carbon ([http://wiki.seas.harvard.edu/geos-  
7 chem/index.php/Aerosol\\_optical\\_properties](http://wiki.seas.harvard.edu/geos-chem/index.php/Aerosol_optical_properties)). In the Advanced Particle Microphysics (APM)  
8 module of GEOS-Chem, hygroscopicity is again parameterized based on Köhler theory (Yu et  
9 al., 2012). When water uptake by both inorganic and organic components is taken into account in  
10 these large-scale chemical transport models, total aerosol liquid water concentrations are  
11 commonly calculated either assuming particles are externally mixed or using a volume- or mass-  
12 weighted average of the  $\kappa$  values or water contents of all simulated components (Drury et al.,  
13 2008; Fu et al., 2012). This simplified treatment of water uptake leads to substantial uncertainties  
14 in predicted direct and indirect radiative forcing of atmospheric aerosols (Chung and Seinfeld,  
15 2002; Kanakidou et al., 2005; Liu and Wang, 2010). Further, the assumption of external or  
16 additive mixing of the aerosol components fails to account for the influence that particle mixing  
17 state and particle-phase morphology can have on aerosol hygroscopicity and optical properties.

18         Recent work has demonstrated that organic and mixed organic-inorganic particles can  
19 exist in multiple phase states depending on their chemical composition and on ambient  
20 conditions such as RH and temperature (Cappa et al., 2008; Zobrist et al., 2008; Ciobanu et al.,  
21 2009; Virtanen et al., 2010; Bertram et al., 2011; Koop et al., 2011; Krieger et al., 2012). For  
22 example, non-ideal interactions between aerosol components can result in a liquid-liquid phase  
23 separation (LLPS) in which an inorganic-electrolyte-rich phase and an organic-rich phase co-  
24 exist within a single particle (Erdakos and Pankow, 2004; Ciobanu et al., 2009; Zuend et al.,  
25 2010; Bertram et al., 2011; Pöhlker et al., 2012; Song et al., 2012a; Zuend and Seinfeld, 2012;  
26 You et al., 2012, 2013, 2014). Laboratory studies have demonstrated that ambient OA can exist  
27 as a highly viscous liquid, semi-solid, or glass under atmospherically relevant conditions (Zobrist  
28 et al., 2008, 2011; Mikhailov et al., 2009; Koop et al., 2011; Tong et al., 2011). Amorphous solid  
29 (glassy) SOA has been observed both in a laboratory chamber and in the field (Virtanen et al.,  
30 2010; Saukko et al., 2012). Such complex phase behavior has major implications for the  
31 partitioning of water and semi-volatile organic species to the particle phase (Ciobanu et al., 2009;

1 Koop et al., 2011; Krieger et al., 2012; Mikhailov et al., 2009; Bones et al., 2012; Song et al.,  
2 2012a, 2014; Zaveri et al., 2014). Diffusion coefficients in solid or semi-solid particles have been  
3 estimated to be up to seven orders of magnitude smaller than in liquids (Vaden et al., 2011;  
4 Abbatt et al., 2012), resulting in the inhibition of mass transfer through the aerosol bulk and  
5 delayed uptake and evaporation of water (Koop et al., 2011; Bones et al., 2012; Shiraiwa et al.,  
6 2011, 2013; Lienhard et al., 2014). Assuming that multi-component particles exist as well-  
7 mixed, single phase liquids when two separate phases are actually present can result in errors as  
8 large as 200% in predicted particle mass formed through the partitioning of organic vapors to the  
9 condensed phase (Zuend et al., 2010; Zuend and Seinfeld, 2012). The present study explores the  
10 extent to which phase separations and other complex phase behavior influence the partitioning of  
11 water vapor to the particle phase.

12 A variety of methods have been used to characterize the factors that influence the  
13 prevalence of LLPS and amorphous solid OA. Coupling single-particle techniques with  
14 microscopy has enabled the observation of particle phase transitions with changing ambient  
15 conditions (Krieger et al., 2012). Song et al. (2012a), for example, evaluated the prevalence of  
16 LLPS as a function of RH and characterized the chemical composition of phases present within  
17 mixed organic-inorganic aerosols using a high-speed video camera and Raman microscopy.  
18 Moisture-induced glass transitions have been observed for sucrose solutions using single particle  
19 techniques and differential scanning calorimetry (Zobrist et al., 2008, 2011). Similarly, phase  
20 states (solid/semi-solid versus liquid) of SOA as a function of RH have been inferred based on  
21 the fraction of particles that bounced when impacted on a steel substrate (Sauuko et al., 2012). A  
22 combination of bounce-fraction measurements and electron microscopy of newly formed OA in  
23 a boreal forest provided the first evidence that SOA formed in the atmosphere can behave as  
24 amorphous solids (Virtanen et al., 2010). These analyses have also shown that phase separation  
25 and particle viscosity vary with chemical composition (e.g., the organic:inorganic mass ratio),  
26 the molecular properties of the organic fraction of the aerosols (e.g., oxygen:carbon [O:C] ratio,  
27 molar mass, hydrophilicity), and RH (Bertram et al., 2011; Song et al., 2012a, b; You et al.,  
28 2013). While these studies have provided valuable information regarding the influence of RH  
29 and particle water content on particle phase state, investigations of the influence of complex  
30 phase behavior on water uptake are limited. Further, the single-particle techniques commonly  
31 used to study particle-phase morphology generally require particle sizes on the order of 1 – 10

1  $\mu\text{m}$  (Krieger et al., 2012). There is a need for the study of the properties and behavior of  
2 submicrometer particles with complex phase morphologies. Herein, we explore variability in the  
3 hygroscopic behavior of accumulation-mode particles with phase morphologies ranging from  
4 well-mixed liquids, to phase-separated particles, to amorphous solids or semi-solids and evaluate  
5 the importance of accounting for such complex phase states and related phase transitions when  
6 modeling water uptake.

7

## 8 **2 Methods**

### 9 **2.1. Hygroscopic Growth Factor Measurements**

10 Diameter hygroscopic growth factors of nine laboratory-generated aerosol systems that  
11 serve as atmospheric aerosol surrogates were measured at RHs ranging from 40 to 90% with the  
12 Differential Aerosol Sizing and Hygroscopicity Spectrometer Probe (DASH-SP). The DASH-SP  
13 has been described in detail previously (Sorooshian et al., 2008). Briefly, in the DASH-SP,  
14 aerosols are dried in a Nafion dryer, pass through a  $^{210}\text{Po}$  neutralizer, and are then size-selected  
15 with a differential mobility analyzer, resulting in a monodisperse aerosol population. The size-  
16 selected aerosols are split into four flows in which they are exposed to humidified air in parallel  
17 Nafion humidifiers at four different, controlled RH values. Residence times in the Nafion dryer  
18 and in each of the humidifiers are 1 s and 4 s, respectively. The aerosols were also sent through a  
19 silica gel diffusion dryer with a residence time of  $\sim 3 - 5$  s prior to entering the DASH-SP. The  
20 size distributions of the particles following humidification are measured with four dedicated  
21 optical particle counters (OPCs). A data processing algorithm that accounts for the dependence  
22 of the OPC signal on particle diameter and refractive index has been developed to calculate wet  
23 particle diameter (i.e., particle diameter after exposure to humidified air) from the OPC signal  
24 (Sorooshian et al., 2008). This calculation requires knowledge of the refractive index of the dry  
25 particle. One of the flow regions of the DASH-SP is kept dry ( $\text{RH} < 8\%$ ) to enable calculation of  
26 the effective refractive index using an empirical relationship between OPC signal height,  
27 refractive index, and particle size. This empirical relationship was developed using calibration  
28 salts with known refractive indices (Sorooshian et al., 2008). It is assumed that the particles are  
29 spherical and that they scatter, but not do absorb, light. Hygroscopic diameter growth factors are  
30 calculated as the ratio of the mode diameter of the wet particle size distribution (i.e., at a 40% –  
31 90% RH set point) to the dry mode particle diameter ( $\text{HGF} = D_{\text{wet}}/D_{\text{dry}}$ ). In this work, HGFs were

1 measured for particles with dry mobility diameters of 250 nm. HGF measurements were  
2 performed at room temperature (~298 K). A minimum of 1500 particles were counted and sized  
3 at each RH value to produce the dry and wet size distributions. Experiments were repeated ten  
4 times for each aerosol system and reported growth factors were calculated as the average across  
5 those ten runs. The overall average uncertainty in DASH-SP-measured HGFs is approximately  
6 5%, but can approach 8% at lower values of RH (Sorooshian et al., 2008).

7         With the aim of exploring the extent to which water uptake varies with particle phase  
8 state, hygroscopic growth curves were measured for chemical systems for which particle phase  
9 behavior as a function of RH has previously been characterized. For all systems studied here,  
10 RH-dependent phase states had previously been observed at room temperature. Most of those  
11 studies were based on single-particle techniques, in which a single-particle (typically  
12 supermicron-sized) is isolated in a controlled environment and probed with various optical and  
13 microscopy techniques (Tong et al., 2011; Zobrist et al., 2011; Song et al., 2012a; You et al.,  
14 2013). Briefly, You et al. (2013) explored the prevalence of liquid-liquid phase separations as a  
15 function of RH for internally mixed organic-inorganic aerosol systems comprising one organic  
16 compound and one inorganic salt. Single particles were deposited on a glass slide coated with a  
17 hydrophobic substrate that was then mounted in a RH- and temperature-controlled flow cell.  
18 Phase transitions during RH cycling were observed with an optical reflectance microscope. Song  
19 et al. (2012a) studied the phase behavior of more complex particle mixtures, each consisting of  
20 three dicarboxylic acids with 5, 6, or 7 carbon atoms ( $C_5$ ,  $C_6$ ,  $C_7$ ) and ammonium sulfate,  
21 deposited on a glass slide using a Raman microscope equipped with a high-speed camera.  
22 Zobrist et al. (2011) and Tong et al. (2011) studied the phase-state and water-uptake behavior of  
23 sucrose particles using an electrodynamic balance coupled with various optical techniques and  
24 optical tweezers coupled with brightfield imaging, respectively.

25         Seven aerosol systems with RH-dependent phase morphologies ranging from well-mixed  
26 liquids, to phase-separated particles, to amorphous solids or semi-solids were chosen for study in  
27 the present work from the above-described studies. Table 1 summarizes the compositions and  
28 phase behaviors of these chemical systems as determined in these prior studies. Two additional  
29 chemical systems consisting of sucrose and ammonium sulfate with varying organic:inorganic  
30 ratios were also studied here. A concurrent study (Robinson et al., 2014) also explored the  
31 hygroscopic behavior of submicron sucrose-ammonium sulfate particles, with the aim of

1 characterizing the influence of glassy aerosol components on the optical properties of organic-  
2 inorganic particles. Sucrose was selected as a model compound in that work and in the present  
3 study due to its high glass-transition temperature ( $T_g = 331 - 335.7$  K), as characterized by  
4 Zobrist et al., (2008) and Dette et al. (2014). The phase behavior of these systems as a function  
5 of RH, however, has only been characterized for a sucrose:ammonium sulfate dry mass ratio of  
6 2:1 (You and Bertram, 2015, Table1). The phase behavior of the 1:1 sucrose-ammonium sulfate  
7 system has not been characterized with single-particle techniques.

8 In addition to differences in phase behavior, the aerosol systems represent variations in  
9 their complexity (in terms of dry composition). Particle compositions range from single-  
10 component organic systems, to two-component systems consisting of one organic and  
11 ammonium sulfate, to more complex systems consisting of dicarboxylic acid mixtures and  
12 ammonium sulfate (Table 1). To evaluate the performance of the DASH-SP and the HGF-  
13 calculation algorithm, control runs were also performed for pure ammonium sulfate aerosols. For  
14 all chemical systems, aerosols were generated by atomizing aqueous solutions prepared by  
15 dissolving the organic and inorganic components with the mass ratios given in Table 1 in Milli-Q  
16 water (resistivity  $\geq 18.2$  M $\Omega$  cm). Ammonium sulfate (purity  $\geq 99\%$ ) and ACS reagent grade  
17 sucrose were purchased from Macron Fine Chemicals; all other organic components were  
18 purchased from Sigma-Aldrich (purity  $\geq 98\%$ ).

## 19 **2.2 Modeling Hygroscopic Growth**

20 Hygroscopic growth curves were modeled for the nine aerosol systems with the Aerosol  
21 Inorganic-Organic Mixtures Functional groups Activity Coefficients (AIOMFAC) model (Zuend  
22 et al., 2008, 2010, 2011; Appendix A). AIOMFAC is a thermodynamic model that explicitly  
23 accounts for molecular interactions between all components in an aqueous solution through the  
24 calculation of activity coefficients. A group-contribution concept based on UNIFAC (UNIversal  
25 quasi-chemical Functional group Activity Coefficients), in which the thermodynamic properties  
26 of organic compounds are determined on the basis of their molecular structures, is employed to  
27 account for interactions between organic functional groups, inorganic ions, and water (Zuend et  
28 al., 2008, 2011). In these AIOMFAC-based equilibrium calculations, the potential existence of a  
29 LLPS is determined and corresponding liquid-phase compositions are computed by the method  
30 of Zuend and Seinfeld (2013). Diameter growth factors are calculated for RH values ranging



1 from near 0 to 99% for both dehydration (from high RH to low RH) and hydration (low RH to  
2 high RH) cycles for all systems. For dehydration-branch calculations, growth factors at RH  
3 values lower than the particle/inorganic salt deliquescence point are representative of metastable  
4 conditions, where a supersaturated solution is present with respect to the dissolved inorganic salt.  
5 Hydration calculations include the presence of a solid inorganic phase at RH values before the  
6 full deliquescence of ammonium sulfate and the partial dissolution of ammonium sulfate into the  
7 aqueous organic solution (solid-liquid equilibrium; SLE). The hydration calculations are the  
8 most relevant to the hygroscopic growth experiments, as the atomized aerosols were dried before  
9 being exposed to elevated humidities in the DASH-SP. AIOMFAC-calculated diameter growth  
10 factors are compared to measured values to provide a detailed evaluation of the interactions  
11 likely to be occurring between aerosol chemical components.

12         Following Zuend and Seinfeld (2012), in addition to the full AIOMFAC-based  
13 equilibrium calculations, several simplified calculations were performed to explore the influence  
14 of phase separation and the effects of other non-ideal interactions on hygroscopic growth. These  
15 comparisons also evaluate the need for accounting for such interactions in modeling the water-  
16 uptake behavior of atmospheric aerosols. Two hygroscopic growth calculations in which no  
17 LLPS was allowed to occur were performed: (1) one in which non-ideal interactions are taken  
18 into account through AIOMFAC-calculated activity coefficients and (2) one in which it is  
19 assumed that the condensed phase behaves as an ideal mixture. Water-uptake calculations were  
20 also performed in a mode in which complete separation between an aqueous inorganic  
21 electrolyte phase and an organic phase is assumed and, thus, no organic-ion interactions are  
22 accounted for. This latter case is similar to a Zdanovskii-Stokes-Robinson (ZSR) relation  
23 assumption, since the water uptake of individual components (here two separate phases) are  
24 added up to estimate the HGF. In our ZSR-like calculation case, the influence of non-ideality on  
25 water activity and, therefore water content, is accounted for within the individual phases with  
26 AIOMFAC-based activity coefficients. A calculation in which a solid organic phase is assumed  
27 at all RH values was also performed for comparison against the DASH-SP measurements in  
28 order to evaluate whether the presence of a solid organic phase was likely in any of the chemical  
29 systems studied. All growth-curve calculations were performed at 298 K.

30         Note that AIOMFAC predicts phase compositions, which can be used to derive mass  
31 growth factors, but not the densities of the phases necessary to calculate diameter growth factors

1 (assuming spherical particles). Solid and liquid-state densities of ammonium sulfate were taken  
2 from Clegg and Wexler (2011). The density of citric acid was calculated based on the data and  
3 parameterizations of Lienhard et al. (2012). The densities of all other organic compounds were  
4 estimated using the structure-based method of Girolami (1994) with the online density-  
5 calculation tools available on the E-AIM website (<http://www.aim.env.uea.ac.uk/aim/aim.php>).  
6 Densities of mixtures within particles and those of individual phases were calculated assuming  
7 additive molar volumes of each component (i.e., ideal mixing in terms of density). Organic  
8 component densities are given in Table 1.

9

## 10 **3 Results and Discussion**

### 11 **3.1 Experimental Hygroscopic Growth Curves and AIOMFAC Modeling**

#### 12 **3.1.1 Two-Component Carboxylic Acid-Ammonium Sulfate Systems**

13 Measured and AIOMFAC-predicted HGFs for the two-component carboxylic acid-  
14 ammonium sulfate systems (organic:inorganic dry mass ratios = 2:1) are shown in Fig. 1. Panels  
15 below the hygroscopic growth curves illustrate AIOMFAC predictions of the occurrence of  
16 phase separation and the composition of each phase. All of the two-component carboxylic acid-  
17 ammonium sulfate systems demonstrate suppressed water uptake at high RH values as compared  
18 to pure ammonium sulfate (Fig. 1a – 1c; Fig. B1). This is expected because, based on  
19 approximately linear additivity in water uptake by the different particle components, a lesser  
20 degree of water uptake by the organic fraction in comparison to inorganic salts (per unit mass) is  
21 typically the case. At RH = 80%, ratios of the HGFs for the mixed organic-inorganic aerosols to  
22 those for pure ammonium sulfate were 0.88, 0.86, and 0.89 for the systems containing  
23 diethylmalonic acid, 2-methylglutaric acid, and citric acid, respectively. Similarly, these values  
24 were 0.90, 0.88, and 0.88 at RH = 90%. At low to moderate RH values (40 – 70%), however, the  
25 shapes and characteristics of the growth curves vary across the systems due, at least in part, to  
26 differences in phase behavior, as is discussed below.

27 Mixed diethylmalonic acid-ammonium sulfate particles demonstrated little to no water  
28 uptake (HGF  $\approx$  1.0) before the particle deliquesced at an RH of approximately 80% (Fig. 1a).  
29 This suggests the presence of a viscous semi-solid, an amorphous solid, or a crystalline solid

1 organic phase (with no water uptake on the timescale of the 4 s residence time in the humidifier).  
2 The presence of a solid organic at low to moderate RH is supported by a comparison between  
3 measured and AIOMFAC-calculated growth factors. For  $RH = 40 - 70\%$ , model-measurement  
4 agreement is closest for the case in which diethylmalonic acid is assumed to be solid. Measured  
5 values then approach the full equilibrium AIOMFAC calculation in which the organic is  
6 assumed to be in a liquid state. Note that all AIOMFAC-based calculations shown by the solid  
7 curves assume that the organic compounds are in a liquid-like state at all RH levels. For this  
8 system, AIOMFAC predicts a SLE state, with diethylmalonic acid dominating the liquid phase  
9 and with the solid phase fully comprised of ammonium sulfate. Following the deliquescence of  
10 ammonium sulfate at  $RH = 79.75\%$ , the particle is predicted to undergo LLPS. The organic-  
11 dominated and the ammonium sulfate-dominated phases are then predicted to merge to a single  
12 phase at  $RH = 94\%$ . The AIOMFAC-predicted RH at which merging of the two phases occurs is  
13 5% higher than that observed by You et al. (2013). It is likely that this small discrepancy can be  
14 attributed to uncertainty in modeled organic-ion interactions. However, it is also possible that  
15 optical methods cannot discern the presence of two phases at  $RH \geq 89\%$  if one of the two  
16 predicted liquid phases is small in mass or volume compared to the other phase.

17 In addition, You et al. (2013) performed dehydration experiments to explore the onset of  
18 phase separation (from high to low RH), while the present study focused on hydration  
19 experiments (from low to high RH). AIOMFAC predictions are made under the assumption that  
20 there is no hysteresis between LLPS and the merging of two liquid phases to a single phase in  
21 terms of the onset RH. This is because experiments (e.g., Song et al., 2012a) show that there is  
22 little to no hysteresis in such a phase transition, at least for systems with liquid-like viscosities. In  
23 contrast to the typical hysteresis behavior of liquid-crystal/crystal-liquid phase transitions (i.e.,  
24 deliquescence vs. crystallization), liquid-liquid to single-liquid phase transitions involve only  
25 disordered phase states (rather than crystalline solids with long-range order). Exceptions to this  
26 may exist for some systems in a particular composition range involving the metastable region of  
27 a liquid-liquid equilibrium phase diagram (e.g. Zuend et al., 2010). However, the energy barrier  
28 for the nucleation and growth of a new liquid phase is small in comparison to the larger energy  
29 barrier that needs to be overcome when a new crystalline phase is formed. Because the merging  
30 of the phases is predicted to occur at an RH at which aqueous diethylmalonic acid is expected to

1 be of low viscosity (Figure 1a), no hysteresis behavior is expected. Thus, we do not expect that a  
2 hysteresis behavior influenced the disagreement in the RH of phase merging discussed above.

3 Like the diethylmalonic acid-ammonium sulfate system, the 2-methylglutaric-containing  
4 aerosols demonstrate a marked increase in water uptake at  $\text{RH} = 80\%$ ; however, more gradual  
5 and continuous water-uptake was observed prior to particle deliquescence (Fig. 1b). Good  
6 agreement was achieved between measured and AIOMFAC-predicted growth curves at all RH  
7 values. AIOMFAC again predicts a SLE state prior to the deliquescence of ammonium sulfate at  
8  $\text{RH} = 79.25\%$ . This is followed by the presence of two liquid phases before full merging of the  
9 phases into a single liquid phase at  $\text{RH} = 82.25\%$ . As was true for the diethylmalonic acid-  
10 ammonium sulfate system, this LLPS phase transition value is higher than the RH of 75%  
11 observed by You et al. (2013). As noted above, this could be related to uncertainty associated  
12 with the parameterization of the AIOMFAC group-contribution method. In addition, with the  
13 gradual merging of the phases, it is possible that a remaining LLPS was not visible in the  
14 experiments at  $\text{RH} > 75\%$ . Again, as is explained above, no hysteresis is expected for the phase  
15 separation and merging for hydration and dehydration conditions for this system.

16 For the citric acid-ammonium sulfate particles, measured growth factors suggest gradual,  
17 continuous water uptake at all experimental RH values (Fig. 1c). This is in agreement with  
18 measurements for this system at different dry organic:inorganic ratios reported by Zardini et al.,  
19 (2008). The AIOMFAC-predicted growth curve indicates a small increase in slope with the  
20 deliquescence of ammonium sulfate at  $\text{RH} = 70.25\%$ , lower than that for pure ammonium  
21 sulfate. This is expected in the presence of a hygroscopic organic compound like citric acid ( $\text{O:C}$   
22 = 1.17) due to the partial solubility of ammonium sulfate in the aqueous, citric acid-rich phase.  
23 Measured and predicted growth factors are in very good agreement at all RH values. For this  
24 system, a single, well-mixed liquid phase is predicted following the complete deliquescence of  
25 ammonium sulfate. This is in agreement with the experimental results of You et al. (2013) and  
26 Bertram et al. (2011), who observed no evidence of LLPS for citric acid-ammonium sulfate  
27 particles.

28 A comparison of hygroscopic growth curves across the three two-component systems  
29 suggests that growth curve shape reflects phase behavior in mixed organic-ammonium sulfate  
30 systems. Growth curves approach smoother, more continuous water uptake with decreasing

1 prevalence of LLPS (i.e., looking from left to right for Fig. 1, panels a – c). In addition to higher  
2 miscibility of the aerosol components for particles with no LLPS or those for which LLPS  
3 persists for only a small range of RH values, this can likely be attributed to the fact that both the  
4 prevalence of LLPS and aerosol hygroscopicity vary with the O:C ratios of the organic  
5 components of mixed organic-inorganic particles (Massoli et al., 2010; Bertram et al., 2011;  
6 Duplissy et al., 2011; Song et al., 2012a; You et al., 2013). Note that the O:C ratios of  
7 diethylmalonic, 2-methylglutaric, and citric acid are 0.57, 0.67, and 1.17, respectively. Thus, the  
8 smoothing of the growth curves with increasing O:C (and, incidentally, lower prevalence of  
9 LLPS) is consistent with the higher propensity of the more polar compounds to take up water and  
10 dissolve some ammonium sulfate (in a SLE) at lower RH.

### 11 **3.1.2 Complex Mixed Dicarboxylic Acid-Ammonium Sulfate Systems**

12 In general, water-uptake behavior was similar across the more complex dicarboxylic  
13 acid-ammonium sulfate mixtures, regardless of the carbon number of the acids included in the  
14 system and the differences in the phase morphologies of the particles observed previously in  
15 experiments by Song et al., (2012a). All systems demonstrated gradual water uptake with growth  
16 factors increasing from 1.0 to ~1.05 prior to a rapid increase in particle diameter of ~30 - 45% at  
17  $RH \approx 80\%$  (Fig. 2). This is in agreement with the results of Song et al. (2012a), who observed  
18 nearly complete or complete particle deliquescence at RH values of 79 - 80% for all three  
19 systems. At  $RH \geq 80\%$ , suppressed hygroscopic growth as compared to ammonium sulfate is  
20 evident, but to a lesser degree than for the two-component systems discussed above, with  
21 reductions in diameter growth factors ranging from 1% to 7%. This is likely attributable to the  
22 smaller organic:inorganic ratios of these systems as compared to the two-component systems  
23 (dry mass ratios of 1:1 rather than 2:1). In addition, mixing effects due to the presence of  
24 multiple organics, which can inhibit crystallization (Cruz and Pandis, 2000, Marcolli et al.,  
25 2004), likely influenced the water uptake behavior of these systems. One constituent of the  $C_7$   
26 acid mixture, diethylmalonic acid, demonstrated behavior indicative of the presence of a  
27 crystalline solid or highly viscous organic phase in the two-component mixture discussed above.  
28 In the more complex  $C_7$  acid mixture, however, it is possible that there is limited, but more  
29 gradual water uptake at low to moderate RH, suggesting a liquid (perhaps moderately viscous)  
30 phase. Owing to their complexity, the multi-acid aerosol systems may provide a better analog for  
31 the majority of mixed organic-inorganic atmospheric aerosols than the two-component systems.

1 As was true for the two-component carboxylic acid-ammonium sulfate systems, we observed a  
2 smoothing of the growth curves with increasing O:C ratio of the C<sub>5</sub>, C<sub>6</sub>, and C<sub>7</sub> dicarboxylic acid  
3 mixtures (O:C = 0.80, 0.67, 0.57, respectively).

4 As determined both through previous experimental work and with the AIOMFAC  
5 modeling, there is variability in phase behavior across the mixed dicarboxylic acid-ammonium  
6 sulfate aerosol systems. For the C<sub>5</sub> dicarboxylic acid-ammonium sulfate system, AIOMFAC  
7 predicts a SLE state of ammonium sulfate prior to complete deliquescence at RH = 77% (Fig.  
8 2a). At this point, ammonium sulfate fully dissolves into the organic-dominated liquid phase. For  
9 the C<sub>6</sub> and C<sub>7</sub> systems, however, AIOMFAC predicts LLPS following the complete  
10 deliquescence of ammonium sulfate at RH = 79.25 and 79.75%, respectively (Figs. 2b, 2c). For  
11 the C<sub>6</sub> system, the inorganic- and organic-dominated phases are then predicted to merge to a  
12 single phase at RH = 83%, while LLPS persists up to RH = 92.75% for the C<sub>7</sub> system.  
13 AIOMFAC predictions of phase behavior are in qualitative agreement with the observations of  
14 Song et al. (2012a). In agreement with AIOMFAC predictions of particle phase state during the  
15 humidification process (i.e., starting from dry conditions), no evidence of LLPS was observed  
16 for the C<sub>5</sub> system (Song et al., 2012a). Contrary to the experiments reported by Song et al.  
17 (2012a), AIOMFAC does predict LLPS at RH values below 80% for the dehydration process of  
18 the C<sub>5</sub> system (i.e., when no solid ammonium sulfate phase is allowed to form). For both the C<sub>6</sub>  
19 and C<sub>7</sub> systems, AIOMFAC overpredicts the RH at which separated phases merge to a single  
20 phase by 10% and 3%, respectively, in comparison to the observations by Song et al. (2012a).  
21 Song et al. (2012a) also observed differences in the morphology of the LLPS states of the C<sub>6</sub> and  
22 C<sub>7</sub> systems. For the C<sub>6</sub> system, an ammonium sulfate core was partially engulfed by an organic-  
23 dominated outer phase containing ammonium sulfate satellite inclusions. The C<sub>7</sub> system  
24 displayed a distinct, fully engulfed core-shell morphology. Despite the small degree of model-  
25 experiment disagreement in the RHs at which merging of two liquid phases occur in the C<sub>6</sub> and  
26 C<sub>7</sub> systems, good agreement between measured and AIOMFAC-predicted growth curves is  
27 achieved for the C<sub>5</sub>, C<sub>6</sub>, and C<sub>7</sub> systems (Figures 2a - c). This suggests that the presence or  
28 absence of LLPS, as well as the morphology of LLPS (which is not taken into account in  
29 AIOMFAC), might influence water-uptake to a lesser degree than other thermodynamic  
30 properties. This is explored subsequently when we compare various modeling methods that vary  
31 in the degree to which they consider thermodynamic non-ideality and LLPS.

### 1 3.1.3 Sucrose-Containing Aerosols

2 The pure sucrose aerosols demonstrate continuous, but limited, water uptake with growth  
3 factors reaching only 1.25 at RH = 90% (Figure 3a). Consequently, as RH approaches 100%, the  
4 growth factor is expected to show a steep increase. Such a steep increase is predicted by the  
5 AIOMFAC-based equilibrium model at RH  $\approx$  95%. For RH  $\leq$  50%, average measured values of  
6 HGF fall below the equilibrium calculations of AIOMFAC; however, this deviation is within  
7 experimental uncertainty. Previous studies demonstrated that the glass transition RH of sucrose  
8 droplets at room temperature ( $\sim$  298 K) ranges between 25 and 53%, depending on the rate of  
9 dehumidification (Zobrist et al., 2011; Tong et al., 2011). Thus, it is possible that a glass  
10 transition occurred with the rapid drying of the atomized sucrose droplets (total residence time in  
11 the silica gel diffusion and Nafion dryers  $\sim$  5 s). However, no quantitative conclusions can be  
12 drawn about the extent to which this affected HGFs in our measurements. Nevertheless, such a  
13 glass transition may have influenced the growth factor measurement at RH < 53 % and could  
14 partially explain the observed discrepancy between the measured and modeled growth factors at  
15 those RH levels. Measured HGFs are in agreement with equilibrium-condition measurements  
16 and modeling of Tong et al. (2011) and Zobrist et al (2011), as well as AIOMFAC-modeled  
17 HGFs, particularly at RH  $\geq$  60%.

18 Like pure sucrose, the sucrose-ammonium sulfate systems demonstrate continuous water-  
19 uptake behavior, with smaller HGFs as compared to pure ammonium sulfate at RH = 80 and  
20 90% (Fig. 3b,c). The magnitude of the deviations in HGF for the sucrose-ammonium sulfate  
21 particles from those for pure ammonium sulfate varies with the organic:inorganic ratio, but is  
22 within the range observed for the other aerosol systems. At RH = 80%, ratios of the HGFs for the  
23 sucrose-ammonium sulfate particles to those for pure ammonium sulfate were 0.86 and 0.91 for  
24 the 2:1 and 1:1 sucrose-ammonium sulfate systems, respectively. These values were 0.85 and  
25 0.89 at RH = 90%.

26 Evidence for the influence of a highly viscous phase state on hygroscopic behavior is  
27 stronger for the mixed sucrose-ammonium sulfate aerosols. While for stable thermodynamic  
28 equilibrium AIOMFAC predicts distinct deliquescence behavior at RH = 80% for both  
29 organic:inorganic ratios, we observed smooth, continuous water uptake for RH = 40 – 90% in the  
30 DASH-SP experiments (Figure 3b, c). Note that before entering the DASH-SP, particles were

1 dried after atomization from a solution, at which point ammonium sulfate crystallization may  
2 occur. Since the viscosity of the solution is expected to increase considerably toward lower RH,  
3 however, the high viscosity (potentially accompanied by a glass transition) may suppress the  
4 crystallization of ammonium sulfate in these systems. The corresponding AIOMFAC  
5 calculations for the humidification process are shown by the solid curves in Fig. 3 (where  
6 ammonium sulfate is in a crystalline state at low RH), while the dashed curves show the model  
7 predictions of HGF for the case where both sucrose and ammonium sulfate are present in a liquid  
8 (potentially viscous) solution. This latter scenario is often observed experimentally during a  
9 dehydration process (starting at very high RH with a homogenous liquid solution). The measured  
10 HGFs are in good agreement with the metastable conditions of the AIOMFAC-modeled  
11 “dehydration branch.” This is in agreement with the results of Robinson et al. (2014), who also  
12 observed continuous water uptake and evidence for the inhibition of the crystallization of  
13 ammonium sulfate in the presence of viscous sucrose. Minor differences ( $\leq 10\%$ ) in the HGFs  
14 reported in their work (RH = 60 – 80%) and those described here can likely be attributed to  
15 differences in technique, as they derived growth factor based on light extinction using Mie  
16 theory, or variances in particle drying and/or humidification times (humidification residence time  
17 = 1 s versus 4 s in this work). Our results suggest that rapid particle drying within HGF  
18 instrumentation can induce a steep increase in particle viscosity, potentially even leading to a  
19 glass transition. As a result, such measurements may not accurately reflect the equilibrium water-  
20 uptake behavior of viscous particles. This has implications for the measurement of HGFs for  
21 ambient aerosol such as the highly oxygenated SOA for which sucrose serves as a surrogate in  
22 these experiments.

23         The formation of a highly viscous liquid or semi-solid phase may also lead to kinetic  
24 limitations, affecting the loss of water by evaporation during the drying process prior to  
25 humidification in the DASH-SP. There is increasing evidence from laboratory and field studies  
26 that viscous liquid or semi-solid SOA components may be present in atmospheric aerosol (e.g.,  
27 Virtanen et al., 2010; Vaden et al., 2011; Saukko et al. 2012; Renbaum-Wolff et al. 2013). Thus,  
28 accounting for kinetic limitations to water uptake and release is crucial to accurately modeling  
29 the dynamic hygroscopic behavior of SOA. However, the good agreement between measured  
30 HGFs and the AIOMFAC-based dehydration-branch equilibrium calculations indicates that  
31 water loss was not substantially inhibited during particle drying. If a glassy sucrose shell had



1 formed in these particles and this shell was of sufficient thickness to inhibit water evaporation  
2 during the  $\sim 5$  s residence time in the dryers, the measured effective "dry" reference diameter  
3 would have been affected by the higher water content. This oversized shell would, in turn, affect  
4 all the experimental HGFs obtained at higher RH due to the normalization by the "dry" particle  
5 diameter. If this were the case, HGFs from the experimental data would likely be lower and  
6 discrepancies from the AIOMFAC-based calculations of the dehydration growth curve would be  
7 larger. Another possible factor contributing to model-measurement disagreement for the sucrose-  
8 ammonium sulfate systems is the lower confidence in the treatment of ether groups by  
9 AIOMFAC as compared to functional groups present in the other systems studied here. This is  
10 due to limited experimental data for the development of parameterizations of ether group-ion  
11 interactions (Zuend et al., 2011). This might also contribute to uncertainty in the predicted phase  
12 behavior of the sucrose-ammonium sulfate aerosols, which indicates a SLE prior to the complete  
13 deliquescence of ammonium sulfate at RH = 80%. It is predicted that LLPS then persists up to  
14 RH = 94.25% for both organic:inorganic ratios explored here (Fig. 3b, c). The predicted  
15 occurrence of LLPS for sucrose (O:C = 0.92) contrasts with previous studies that suggest that  
16 LLPS is unlikely for organic compounds with O:C > 0.7 – 0.8 (Bertram et al., 2011; Song et al.,  
17 2012b; You et al., 2013), as well as the experimental results of You and Bertram (2015), in  
18 which no LLPS was observed for sucrose-ammonium sulfate particles with an organic to  
19 inorganic dry mass ratio of 2:1.

### 20 **3.1.4 Measurement and Modeling Limitations and Uncertainty**

21 As noted above, data availability limitations and variability in experimental conditions  
22 for the datasets used in developing parameterizations of functional group-ion interactions in  
23 AIOMFAC contribute to uncertainties in ether-ion interactions and other functional-group-ion  
24 interactions. In addition, other measurement and modeling limitations can contribute to  
25 uncertainty in measured and predicted HGFs. Because experimental data regarding the densities  
26 of organic compounds are limited, the densities of many of the organic compounds studied in  
27 this work were estimated with a group-contribution method (Girolami et al., 1994). Further, for  
28 all aerosol systems and all phases present within the particles, it was assumed that the molar  
29 volumes of the aerosol components are additive (i.e., ideal mixing in terms of volume and  
30 density contributions), regardless of the thermodynamic properties of the mixture under  
31 consideration.

1           Complex particle-phase morphologies can also present unique sources of error and  
2 uncertainty in HGF measurement methods that use optical methods, such as the DASH-SP. For  
3 example, the algorithm that calculates diameter growth factor assumes that the refractive index  
4 of the non-water aerosol components is constant at the value measured in the dry DASH-SP  
5 channel. For systems with non-uniform surfaces (e.g., the C<sub>6</sub> dicarboxylic acid-ammonium  
6 sulfate system, which has been shown to have an organic outer shell with satellite ammonium  
7 sulfate inclusions or partially engulfed morphology; Song et al., 2012a), this assumption might  
8 not be accurate. In addition, the effective refractive index of the organic and inorganic particle  
9 components might evolve upon humidification as previously separated phases merge. This  
10 behavior has the potential to influence hygroscopicity measurements for systems that have core-  
11 shell morphologies at low RH to moderate RH that then transition to a single liquid-phase state  
12 with increasing water content and might contribute to the greater model-measurement  
13 disagreement at RH = 80% observed for the C<sub>7</sub> dicarboxylic acid-ammonium sulfate system.  
14 However, the overall agreement achieved between measured HGFs and AIOMFAC-calculated  
15 values in this work suggests that these factors, and their corresponding uncertainties, are not a  
16 substantial issue for the measurement of HGFs for the aerosol compositions and particle size  
17 range studied here.

18           In addition, as noted above, the DASH-SP HGF experiments were performed with  
19 particles much smaller than those used in the microscopy or electrodynamic balance experiments  
20 that had previously been used to directly characterize LLPS and glass transitions in the particle  
21 systems studied. Thus, the phase behavior of the particles studied here was not characterized  
22 directly. There is some limited evidence that the prevalence of LLPS can vary with particle size.  
23 Veghte et al., (2013) observed that LLPS did occur in larger particles comprised of ammonium  
24 sulfate and succinic acid or pimelic acid (diameters  $\geq 170$  and 270 nm, respectively), but that  
25 LLPS was not evident in smaller particles with the same composition and organic:inorganic mass  
26 ratios. While the DASH-SP experiments do not directly reveal whether a phase separation is  
27 present in the particles, the observed hygroscopic growth in comparison to the model  
28 calculations is in agreement with such phase behavior in the corresponding LLPS RH ranges.  
29 Finally, the timescale of humidification in our experiments differs from that in the single-particle  
30 studies. For example, in the mixed dicarboxylic acid-ammonium sulfate single-particle  
31 experiments, RH was changed at a rate of 0.14 – 0.34% min<sup>-1</sup> (Song et al., 2012). The extent to

1 which the timescale of humidification influences the occurrence of phase separation is unknown;  
2 however, again, agreement between the measured hygroscopic growth and those calculated  
3 under equilibrium conditions suggests humidification timescale did not have a substantial impact  
4 on phase behavior.

### 5 **3.2 Evaluation of Simplified Thermodynamic Assumptions**

6 For the multicomponent systems for which we expect that observed water-uptake  
7 behavior is governed by thermodynamic equilibrium conditions (i.e., excluding the sucrose-  
8 containing systems, which display evidence of kinetic limitations to the crystallization of  
9 ammonium sulfate), we compared the rigorous thermodynamic modeling of the AIOMFAC-  
10 based equilibrium HGF predictions (“AIOMFAC, equilibrium” in Figure 4) to that based on  
11 several simplified thermodynamic assumptions: (1) representing particles as ideal, well-mixed  
12 liquids (“Ideal – well-mixed liquid”), (2) forcing a single liquid phase following the  
13 deliquescence of ammonium sulfate, but accounting for non-ideal interactions through activity  
14 coefficient calculations and allowing for a SLE of ammonium sulfate (“No LLPS – non-ideal”),  
15 and (3) a ZSR-like calculation in which complete separation between the inorganic and organic  
16 components is assumed at all RH levels (“Complete Phase Separation (ZSR)”). Water is the only  
17 component allowed to partition to both phases in this ZSR-like calculation case. In all of these  
18 simplified calculation cases, the formation of a solid ammonium sulfate phase is allowed to exist  
19 (below its deliquescence point at the given temperature), except for the single-phase, ideal  
20 mixture case. We evaluate the extent to which these simple, relatively computationally  
21 inexpensive modeling approaches capture the hygroscopic behavior of particles with varied and  
22 complex phase states. Note that for the diethylmalonic acid-ammonium sulfate system, we first  
23 focus on the calculation for which the presence of a solid organic is predicted prior to particle  
24 deliquescence (“Solid Organic” in Figure 4). At  $RH \geq 80\%$ , we then consider the full AIOMFAC  
25 equilibrium calculation in our discussion of model error, as this offered the best agreement  
26 between measured and modeled values (Figure 1a). For all other systems, we focus on the full  
27 AIOMFAC-based equilibrium calculations at all RH values.

28 Figure 4 shows a comparison between the AIOMFAC-predicted HGFs for the hydration-  
29 branch of a humidity cycle and those calculated with the simplified modeling approaches. The  
30 performance of each of the simplified modeling approaches differs for particles depending on

1 phase state. This suggests that a single simplified modeling approach cannot be used to capture  
2 the water-uptake behavior for the diversity of particle-phase behaviors expected in the  
3 atmosphere. For all systems, except the citric acid-ammonium sulfate particles, the assumption  
4 that the particles could be represented as thermodynamically ideal liquid mixtures leads to the  
5 greatest deviation from AIOMFAC-predicted growth curves. We also note that such  
6 discrepancies depend on the organic:inorganic dry state mass ratios. Generally, the smaller the  
7 ammonium sulfate mass fraction, the lower the degree of hysteresis behavior of  
8 hydration/dehydration processes. Overpredictions of diameter growth factors increase from those  
9 at low RH to a maximum just prior to the rapid increase in water uptake associated with  
10 deliquescence of ammonium sulfate, then drop to within  $\sim 5\%$  of AIOMFAC values (Fig. 4).  
11 Maximum errors for the assumption of ideality ranged from 10 – 26% and increased with  
12 increased prevalence of LLPS (i.e., looking from right to left from Figure 4 panels a - c and from  
13 left to right from panels d – f). For the citric acid-ammonium sulfate system, which does not  
14 undergo LLPS, ideal and AIOMFAC calculated growth curves are in good agreement for  $RH \leq$   
15 80%. Error then increases slightly to  $\sim 5\%$ .

16 Not surprisingly, the forced single-phase calculations, in which non-ideal interactions are  
17 taken into account but LLPS is not, perform well for the  $C_5$  dicarboxylic-ammonium sulfate and  
18 citric acid-ammonium sulfate systems, which demonstrated no LLPS (Figure 4c, d). For these  
19 systems, the ZSR-like calculation leads to largest disagreement, with maximum errors of  
20 between 10 and 18% occurring between RH values of 60 and 80%. This can be attributed to  
21 delayed particle deliquescence in the ZSR-like calculations, since the partial dissolution of  
22 ammonium sulfate in the aqueous organic phase is not considered in this case. Similarly, for  
23 systems for which LLPS persists for only a small range of RH values, the single-phase  
24 assumption performs well, with errors never exceeding 5% (e.g., the 2-methylglutaric-  
25 ammonium sulfate and  $C_6$  dicarboxylic acid-ammonium sulfate systems; Figure 4b, d). The  
26 single-phase assumption also performs well for the systems for which LLPS does occur over a  
27 wider RH range, but delayed prediction of particle deliquescence leads to a large spike in  
28 underprediction of particle diameter at  $RH \approx 80\%$ . The good performance of the single-phase  
29 assumption at most RH values suggests that accounting for LLPS in calculations of hygroscopic  
30 growth might be less important than accounting for other non-ideal interactions between  
31 condensed-phase components. However, this result is likely not applicable to mixed organic-

1 inorganic systems with less water-soluble (i.e., less hygroscopic) organic components, where  
2 LLPS is more prevalent and water uptake by the organic fraction is limited (Zuend and Seinfeld,  
3 2012).

4 For systems that do undergo LLPS, the ZSR-like calculation also performs relatively well  
5 across the range of RH values studied, but displays discrepancies to the AIOMFAC-based  
6 equilibrium prediction of 12 – 18% at moderate RH values due to deviations in the predicted  
7 SLE and deliquescence transition of ammonium sulfate. For these systems, the ZSR-like  
8 calculation also underpredicts water uptake at RH values above the point at which separated  
9 liquid phases merged to a single phase, with relative deviations approaching 10%. As expected,  
10 growth curves begin to converge towards the AIOMFAC equilibrium predictions as RH  
11 approaches 100% for all systems, as the solutions become very dilute (Fig. 4). Our results  
12 suggest that lack of accounting for non-ideal interactions and phase-separations leads to errors in  
13 predicted sub-saturated hygroscopic growth. Note that while maximum deviations in HGFs for  
14 the simplified approaches (compared to the AIOMFAC-based equilibrium calculation) are  
15 generally on the order of 10 – 25%, the corresponding errors in particle size and refractive index  
16 can substantially impact estimates of aerosol scattering and radiative forcing (Finlayson-Pitts and  
17 Pitts, 2000).

18

## 19 **4 Conclusions**

20 Measurements and detailed thermodynamic modeling of the water uptake of model  
21 organic-inorganic atmospheric aerosol systems demonstrate variability in hygroscopic behavior  
22 across aerosol systems with differing RH-dependent phase behavior. Measured and modeled  
23 growth curves approach smoother, more continuous water uptake with decreasing prevalence of  
24 LLPS and increasing O:C ratios of the OA components. AIOMFAC-predicted growth curves  
25 reproduce the measured hygroscopic behavior reasonably well for all systems. A comparison  
26 between measured and modeled HGFs for the sucrose-ammonium sulfate particles indicates the  
27 presence of a viscous semi-solid phase that inhibits the crystallization of ammonium sulfate. We  
28 conclude that particle drying within HGF instrumentation may induce the formation of a highly  
29 viscous, amorphous phase (potentially accompanied by a moisture-loss-related glass transition).  
30 As a result, such measurements may not accurately reflect equilibrium water-uptake behavior.

1 This is an important consideration when applying similar instruments to measure the hygroscopic  
2 behavior of ambient aerosols, particularly for the highly oxygenated SOA for which sucrose  
3 serves as a surrogate in our experiments. Our results add support to the growing body of  
4 literature suggesting that accounting for the influence of viscous liquid or semi-solid phases to  
5 water uptake and release can be important for accurately modeling the hygroscopic behavior of  
6 atmospheric aerosols. The performance of simplified approaches for modeling water uptake  
7 differs for particles with differing phase states/equilibria, suggesting that a single simplified  
8 modeling approach cannot be used to capture the water-uptake behavior for the diversity of  
9 particle phase behavior expected in the atmosphere. Errors in HGFs calculated using the  
10 simplified models are of sufficient magnitude to contribute substantially to uncertainties in  
11 estimates of particle optical and radiative properties. Parameterizations of LLPS and other  
12 complex phase behavior based on commonly measured variables such as O:C (e.g., Bertram et  
13 al., 2011; Koop et al., 2011; Song et al., 2012a) may prove valuable in applying the simplified  
14 HGF calculation approaches explored here in large-scale models. Average carbon oxidation state  
15 ( $\overline{\text{OS}}_C$ ) has also been presented as an indicator of the degree of aerosol oxidation (Kroll et al.,  
16 2011) and may be a useful measure when the goal is to track changes in hygroscopicity with the  
17 progression of oxidation and fragmentation of organic molecules in an atmospheric chemistry  
18 model. Parameterizations of hygroscopicity based on  $\overline{\text{OS}}_C$  might also lead to advancements in the  
19 modeling of aerosol water uptake for complex organic and mixed organic-inorganic systems and  
20 should be a consideration in future work. Finally, while the majority of field-based  
21 hygroscopicity studies focus on relatively high RH values, future measurements could also focus  
22 on the growth factors of atmospheric aerosol at low to moderate RH values, as this is the region  
23 where water-uptake behavior demonstrates the greatest variability with particle-phase behavior.

24

## 25 **Appendix A: AIOMFAC Model and Phase Equilibrium Calculations**

26 AIOMFAC is a group-contribution, thermodynamic model for the calculation of  
27 component activity coefficients in binary and multicomponent mixtures. It was developed to  
28 explicitly account for molecular interactions between organic functional groups and inorganic  
29 ions in aqueous solutions relevant to atmospheric aerosol chemistry. Descriptions of model  
30 details and parameterizations are available elsewhere (Zuend et al., 2008, 2010, 2011; Zuend and

1 Seinfeld, 2012; <http://www.aiomfac.caltech.edu>). Herein, we provide a brief overview of the key  
2 aspects of the AIOMFAC model.

3         Within the model, organic molecules are represented as assemblies of functional groups.  
4 This treatment of organic molecules is based on the concept that the physiochemical properties  
5 of organic compounds can be related to their chemical structure and characteristic structural  
6 groups, which allows for treatment of the hundreds to thousands of organic compounds that  
7 characterize atmosphere organic aerosol. The organic functional groups included in AIOMFAC  
8 (alkyl (standard), alkyl (in alcohols), alkyl (in hydrophobic tails of alcohols), alkyl (bonded to  
9 hydroxyl group), alkenyl, aromatic hydrocarbons, hydroxyl, aromatic carbon-alcohol, ketone,  
10 aldehyde, ester, ether, carboxyl, hydroperoxide, peroxyacid, peroxide (organic), peroxyacyl  
11 nitrate, organonitrate) allow for the representation of a large variety of compounds observed in  
12 atmospheric aerosols. In addition AIOMFAC includes seven atmospherically-relevant cations  
13 ( $H^+$ ,  $Li^+$ ,  $Na^+$ ,  $K^+$ ,  $NH_4^+$ ,  $Mg^{2+}$ ,  $Ca^{2+}$ ), five anions ( $Cl^-$ ,  $Br^-$ ,  $NO_3^-$ ,  $HSO_4^-$ ,  $SO_4^{2-}$ ), and water.

14         Non-ideality (i.e., deviations from Raoult's law) in organic-inorganic aqueous solutions  
15 is accounted for through the calculation of activity coefficients for all components in a given  
16 mixture. When considering the partitioning of water vapor to a multicomponent liquid mixture,  
17 the vapor pressure of water ( $p_w$ ) over the mixture is related to water activity by:

$$18 \quad p_w = p_w^o a_w^{(x)} \quad (A1),$$

19 where  $p_w^o = p_w^o(T)$  is the saturation vapor pressure over pure liquid water at temperature  $T$  and  
20  $a_w^{(x)}$  is the water activity defined on a mole fraction basis. Under thermodynamic equilibrium  
21 conditions, relative humidity and water activity are related by

$$22 \quad RH = a_w^{(x)} = \gamma_w^{(x)} x_w \quad (A2)$$

23 where  $\gamma_w^{(x)}$  is the activity coefficient of water on a mole fraction basis and  $x_w$  is the mole fraction  
24 of water in the particle-phase liquid mixture (here, for the case of a single liquid phase).  
25 Similarly, activity coefficients are key to accurately describing the partitioning of semi-volatile  
26 organic compounds between the gas and particle phases under thermodynamic equilibrium.

27         In AIOMFAC, activity coefficients are derived from expressions for the long-range,  
28 middle-range, and short-range molecular interactions that contribute to total Gibbs excess

1 energy, which is a descriptor of the overall non-ideality of a thermodynamic system. In addition  
2 to their application in calculations of the gas-particle partitioning of water and other semi-  
3 volatile species (i.e., vapor-liquid equilibria), activity coefficients of all components in a multi-  
4 component mixture are required for the calculation of solid-liquid (SLE) and liquid-liquid  
5 equilibria (LLE). The prevalence of liquid-liquid phase separation and the composition of each  
6 phase is calculated in this work by application of AIOMFAC to compute activity coefficients in  
7 distinct liquid phases based on a reliable and efficient algorithm for finding the phase  
8 compositions that correspond to an equilibrium state. A liquid-liquid equilibrium state of a  
9 closed thermodynamic system is a state of minimum Gibbs energy of that system. The same  
10 applies to SLE and, likewise, to coupled vapor-liquid-liquid-solid equilibrium calculations, such  
11 as those performed in this work at given temperature and relative humidity to determine the  
12 number and composition of the particle phases at equilibrium. Hence, while the AIOMFAC  
13 model is at the heart of such equilibrium calculations, the distinct phases and their compositions  
14 are determined using a more general thermodynamic equilibrium model, as described by Zuend  
15 et al. (2010) and Zuend and Seinfeld (2012). For the calculation of a potential liquid-liquid phase  
16 separation, the equilibrium model essentially solves a system of nonlinear equations numerically  
17 to determine the phase state (i.e., one liquid phase versus two liquid phases) that achieves a  
18 minimum in Gibbs energy for a given overall particle-phase composition at constant temperature  
19 and pressure. Full details regarding the algorithm used to diagnose the prevalence of LLPS and  
20 to calculate the corresponding phase composition is available in Zuend and Seinfeld (2013).

21

## 22 **Appendix B: Control Hygroscopic Growth Experiments**

23 Following the same methods as described in the main text of the paper, control  
24 hygroscopic growth experiments were conducted for pure ammonium sulfate aerosols with dry  
25 mobility diameters of 250 nm. HGF experiments were conducted at room temperature (~298 K).  
26 The control experiments were conducted for comparison against the mixed organic-ammonium  
27 sulfate aerosol systems (i.e., to explore the influence of the organic species on the mixed organic-  
28 inorganic particle hygroscopicity when starting with the same dry size) and to evaluate the  
29 performance of the DASH-SP and the growth-factor-calculation algorithm using this well-  
30 characterized aerosol system. DASH-SP measurements reproduced previous experimental



1 characterizations of ammonium sulfate aerosol hygroscopicity (e.g., Tang, 1980; Sorooshian et  
2 al., 2008) and are in agreement with AIOMFAC-predicted diameter growth factors (Figure B1).

3

#### 4 **Author Contributions**

5 N. H., J. H. S., and R. C. F. designed the experiments. N. H. carried out the experiments with  
6 assistance from W. M. A. Z. developed the modeling tools and performed all simulations. N. H.  
7 prepared the manuscript with contributions from all co-authors.

8

#### 9 **Acknowledgements**

10 This work was supported by the National Science Foundation under Award No. 1433246 and the  
11 Office for Naval Research under Award No. N00014-14-1-0097. W. M. was supported by an  
12 NSF Graduate Research Fellowship (Grant No. DGE-1144469) and NSF Grant No. CBET-  
13 1236909. A. Z. was supported by a McGill University Start-up grant.

14

## 1 **References**

- 2 Abbatt, J. P. D., Lee, A. K. Y., and Thornton J.A.: Quantifying trace gas uptake to tropospheric  
3 aerosol: recent advances and remaining challenges, *Chem. Soc. Rev.*, 41, 6555 – 6581,  
4 2012.
- 5 Bertram, A. K., Martin, S. T., Hanna, S. J., Smith, M. L., Bodsworth, A., Chen, Q., Kuwata, M.,  
6 Liu, A., You, Y., and Zorn, S. R.: Predicting the relative humidities of liquid-liquid phase  
7 separation, efflorescence, and deliquescence of mixed particles of ammonium sulfate,  
8 organic material, and water using the organic-to-sulfate mass ratio of the particle and the  
9 oxygen-to-carbon elemental ratio of the organic component, *Atmos. Chem. Phys.*, 11,  
10 10995–1006, 2011.
- 11 Binkowski, F. S. and Roselle, S. J.: Models-3 Community Multiscale Air Quality (CMAQ)  
12 model aerosol component 1. Model description, *J. Geophys. Res.*, 108 4183, doi:  
13 10.1029/2001JD001409, 2003
- 14 Bones, D. L., Reid, J. P., Lienhard, D. M., and Krieger, U. K.: Comparing the mechanism of  
15 water condensation and evaporation in glassy aerosol, *Proc. Natl. Acad. Sci.*, 109, 11613 –  
16 11618, 2012.
- 17 Brooks, S. D., DeMott, P. J., and Kreidenweis, S. M.: Water uptake by particles containing  
18 humic materials and mixtures of humic materials with ammonium sulfate, *Atmos. Environ.*,  
19 38, 1859-1868, 2004.
- 20 Cappa, C. D., Lovejoy, E. R., and Ravishankara, A. R.: Evidence for liquid-like and nonideal  
21 behavior of a mixture of organic aerosol components, *Proc. Natl. Acad. Sci.*, 105, 18687–  
22 18691, 2008.
- 23 Chan, M. N., Choi, M. Y., Ng, N. L., and Chan, C. K.: Hygroscopicity of water-soluble organic  
24 compounds in atmospheric aerosols: amino acids and biomass burning derived organic  
25 species, *Environ. Sci. Technol.*, 39, 1555-1562, 2005.
- 26 Chan, M. N., Lee, A. K. Y., and Chan, C. K.: Responses of ammonium sulfate particles coated  
27 with glutaric acid to cyclic changes in relative humidity: hygroscopicity and Raman  
28 characterization, *Environ. Sci. Technol.*, 40, 6983–6989, 2006.

- 1 Choi, M. Y. and Chan, C. K.: Continuous measurements of the water activities of aqueous  
2 droplets of water-soluble organic compounds, *J. Phys., Chem. A.*, 106, 4566-4572, 2002a.
- 3 Choi, M. Y. and Chan, C. K.: The effects of organic species on the hygroscopic behaviors of  
4 inorganic aerosols, *Environ. Sci. Technol.*, 36, 2422-2428, 2002b.
- 5 Chung, S. H. and Seinfeld, J. J.: Global distribution and climate forcing of carbonaceous  
6 aerosols, *J. Geophys. Res.*, 107, 4407, doi: 10.1029/2001JD001397, 2002.
- 7 Ciobanu, V. G., Marcolli, C., Krieger, U. K., Weers, U., and Peter, T.: Liquid-liquid phase  
8 separation in mixed organic/inorganic aerosol particles. *J. Phys. Chem.*, 113 10966–10978,  
9 2009.
- 10 Clegg, S. L., Seinfeld, J. H., and Brimblecombe, P.: Thermodynamic modeling of aqueous  
11 aerosols containing electrolytes and dissolved organic compounds, *J. Aerosol Sci.*, 32, 713-  
12 738, 2001.
- 13 Clegg, S. L. and Seinfeld, J. H.: Thermodynamic models of aqueous solutions containing  
14 inorganic electrolytes and dicarboxylic acids at 298.25 K. 1. The acids as nondissociating  
15 components, *J. Phys. Chem. A*, 110, 5692-5717, 2006.
- 16 Clegg, S. L. and Wexler, A. S.: Densities and Apparent Molar Volumes of Atmospherically  
17 Important Electrolyte Solutions. 1. The Solutes H<sub>2</sub>SO<sub>4</sub>, HNO<sub>3</sub>, HCl, Na<sub>2</sub>SO<sub>4</sub>, NaNO<sub>3</sub>,  
18 NaCl,(NH<sub>4</sub>)<sub>2</sub>SO<sub>4</sub>, NH<sub>4</sub>NO<sub>3</sub>, and NH<sub>4</sub>Cl from 0 to 50° C, including extrapolations to very  
19 low temperature and to the pure liquid state, and NaHSO<sub>4</sub>, NaOH, and NH<sub>3</sub> at 25° C." *J.*  
20 *Phys. Chem. A*, 115, 3393-3460, 2011.
- 21 Cruz, C., and Pandis, S.N.: Deliquescence and hygroscopic growth of mixed inorganic-organic  
22 atmospheric aerosol. *Environ. Sci. Technol.*, 32, 4313 – 4319, 2000.
- 23 Dette, H. P., Qi, M., Schröder, D. C., Godt, A., and Koop, T.: Glass-forming properties of 3-  
24 methylbutane-1,2,3-tricarboxylic acid and its mixtures with water and pinonic acid. *J. Phys.*  
25 *Chem. A.*, 118, 7024-7033, 2014.
- 26 Drury, E., Jacob, D. J., Wang, J., Spurr, R. J. D., and Chance, K.: Improved algorithm for  
27 MODIS satellite retrievals for aerosol optical depth over western North America, *J.*  
28 *Geophys. Res.*, 113, D16204, doi: 10.1029/2007JD009573, 2008.

1 Duplissy, J., DeCarlo, P. F., Dommen, J., Alfarra, M. R., Metzger, A., Barmapadimos, I., Prevot,  
2 A. S. H., Weingartner, E., Tritscher, T., Gysel, M., Aiken, A. C., Jimenez, J. L.,  
3 Canagaratna, M. R., Worsnop, D. R., Collins, D. R., Tomlinson, J., and Baltensperger, U.:  
4 Relating hygroscopicity and composition of organic aerosol particulate matter, *Atmos.*  
5 *Chem. Phys.*, 11, 1155-1165, 2011.

6 Erdakos, G. B. and Pankow, J. F.: Gas/particle partitioning of neutral and ionizing compounds  
7 to single- and multi-phase aerosol particles. 2. Phase separation in liquid particulate matter  
8 containing both polar and low-polarity organic compounds, *Atmos. Environ.*, 38, 1005 –  
9 1013, 2004.

10 Ervens, B., Turpin, B. J., and Weber, R. J.: Secondary organic aerosol formation in cloud  
11 droplets and aqueous particles (aqSOA): a review of laboratory, field, and model studies.  
12 *Atmos. Chem. Phys.*, 11, 11069-11102, 2011.

13 Ervens, B., Wang, Y., Eagar, J., Leitch, W. R., Macdonald, A. M., Valsaraj, K. T., and  
14 Herckes, P.: Dissolved organic carbon (DOC) and select aldehydes in cloud and fog water:  
15 the role of the aqueous phase in impacting trace gas budgets. *Atmos. Chem. Phys.*, 13,  
16 5117-5135, 2013.

17 Finlayson-Pitts B. J. and Pitts Jr., J. N.: *Chemistry of the Upper and Lower Atmosphere*,  
18 Academic Press, San Diego, CA, 2000.

19 Fu, Y., Luo, G., and Ma, X.: Regional and global modeling of aerosol optical properties with a  
20 size, composition, and mixing state, resolved particle microphysics model, *Atmos. Chem.*  
21 *Phys.*, 12, 5719-5736, 2012.

22 Gao, Y., Yu, L. E., and Chen, S. B.: Effects of organics on the efflorescence relative humidity  
23 of ammonium sulfate or sodium chloride particles, *Atmos. Environ.*, 42, 4433-4445, 2008.

24 Girolami, G. S.: A simple “back of the envelope” method for estimating the densities and  
25 molecular volumes of liquids and solids, *J. Chem. Educ.*, 71, 962-964, 1994.

26 Goldstein, A. H. and Galbally, I. E.: Known and unexplored organic constituents in the Earth’s  
27 atmosphere, *Environ. Sci. Technol.*, 41, 1514-1521, 2007.

- 1 Gysel, M., Weingartner, E., Nyeki, S., Paulsen, D., Baltensperger, U., Galambos, I., and Kiss,  
2 G.: Hygroscopic properties of water-soluble matter and humic-like organics in atmospheric  
3 fine aerosol, *Atmos. Chem. Phys.*, 4, 35-50, 2004.
- 4 Hallquist, M., Wenger, J. C., Baltensperger, U., Rudich, Y., Simpson, D., Claeys, M., Dommen,  
5 J., Donahue N. M., George, C., Goldstein, A. H., Hamilton, J. F., Herrmann, H., Hoffmann,  
6 T., Iinuma, Y., Jang, M., Jenkin, M. E., Jimenez, J. L., Kiendler-Scharr, A., Maenhaut, W.,  
7 McFiggans, G., Mentel, T. F., Monod, A., Prevot, A. S. H., Seinfeld, J. H., Surratt, J. D.,  
8 Szmigielski, R., and Wildt, J.: The formation, properties and impact of secondary organic  
9 aerosol: current and emerging issues, *Atmos. Chem. Phys.*, 9, 5155–5236, 2009.
- 10 Hatch, C. D., Gierlus, K. M, Zahardis, J., Schuttlefield, J., and Grassian, V. H.: Water uptake of  
11 humic and fulvic acid: measurements and modelling using single parameter Köhler theory,  
12 *Environ. Chem.*, 6, 380-388, 2009.
- 13 Kanakidou, M., Seinfeld, J. H., Pandis, S. N., Barnes, I., Dentener, F. J., Facchini, M. C., Van  
14 Dingenen, R., Ervens, B., Nenes, A., Nielsen, C. J., Swietlicki, E., Putaud, J. P., Balkanski,  
15 Y., Fuzzi, S., Horth, J., Moortgat, G. K., Winterhalter, R., Myhre, C. E. L., Tsigaridis, K.,  
16 Vgnati, E., Stephanou, E. G., and Wilson, J.: Organic aerosol and global climate modeling:  
17 a review, *Atmos. Chem. Phys.*, 5, 1053-1123, 2005.
- 18 Koepke, P., Hess, M., Schult, I., and Shettle, E. P: Global Aerosol Data Set, Rep. No. 243, Max-  
19 Planck-Institut für Meteorol., Hamburg, Germany, 1997.
- 20 Koop, T., Bookhold, J., Shiraiwa, M., and Pöschl, U.: Glass transition and phase state of organic  
21 compounds: dependency on molecular properties and implications for secondary organic  
22 aerosols in the atmosphere, *Phys. Chem. Chem. Phys.*, 13, 1923–19255, 2011.
- 23 Krieger, U., Marcolli, C., and Reid, J. P.: Exploring the complexity of aerosol particle  
24 properties and processes using single particle techniques, *Chem. Soc. Rev.*, 41, 6631–6662,  
25 2012.
- 26 Kroll, J. H., Donahue, N. M., Jimenez, J. L., Kessler, S. H., Canagaratna, M. R., Wilson, K. R.,  
27 Altieri, K. E., Mazzoleni, L. R., Wozniak, A. S., Bluhm, H., Mysak, E. R., Smith, J. D.,  
28 Kolb, C. E., and Worsnop, D. R.: Carbon oxidation state as a metric for describing the  
29 chemistry of atmospheric organic aerosol, *Nature Chemistry*, 3, 133-139, 2011.

1 Lei, T., Zuend, A., Wang, W. G., Zhang, Y. H., and Ge, M. F.: Hygroscopicity of organic  
2 compounds from biomass burning and their influence on the water uptake of mixed  
3 organic-ammonium sulfate aerosols, *Atmos. Chem. Phys.*, 14, 111625-11183, 2014.

4 Lienhard, D. M., Bones, D. L., Zuend, A., Krieger, U. K., Reid, J. P., and Peter, T.:  
5 Measurements of thermodynamic and optical properties of selected aqueous organic and  
6 organic-inorganic mixtures of atmospheric relevance, *J. Phys. Chem. A*, 116, 9954-9968,  
7 2012.

8 Lienhard, D. M., Huisman, A. J., Bones, D. L., Te, Y-F., Luo, B. P., Krieger, U. K., and Reid, J.  
9 P.: Retrieving the translational diffusion coefficient of water from experiments on single  
10 levitated aerosol droplets, *Phys. Chem. Chem. Phys.*, 16, 16677-16683, 2014.

11 Liu, X. and Wang, J.: How important is organic aerosol hygroscopicity to aerosol indirect  
12 forcing? *Environ. Res. Lett.*, 5, 044010, doi:10.1088/1748-9326/5/4/044010, 2010.

13 Marcolli, C., Luo, B. P., Peter, Th., and Wienhold, F. G.: Internal mixing of the organic aerosol  
14 by gas phase diffusion of semivolatile organic compounds, *Atmos. Chem. Phys.*, 4, 2593-  
15 2599, 2004.

16 Marcolli, C. and Krieger, U. K.: Phase changes during hygroscopicity cycles of mixed  
17 organic/inorganic model systems of tropospheric aerosols, *J. Phys. Chem. A*, 110, 1881-  
18 1893, 2006.

19 Marcolli, C., Luo, B. P., Peter, Th., and Wienhold, F. G.: Internal mixing of the organic aerosol  
20 by gas diffusion of semivolatile organic compounds, *Atmos. Chem. Phys.*, 4, 2593-2599,  
21 2006.

22 Massoli, P., Lambe, A. T., Ahern, A. T., Williams, L. R., Ehn, M., Mikkilä, J., Canagaratna, M.  
23 R., Brune, W. H., Onasch, T. B., Jayne, J. T., Petäjä, T., Kulmala, M., Laaksonen, A.,  
24 Kolb, C. E., Davidovits, P., and Worsnop, D. R.: Relationships between aerosol oxidation  
25 level and hygroscopic properties of laboratory generated secondary organic aerosol (SOA)  
26 particles, *Geophys. Res. Lett.*, 37, L24801, doi: 10.1029/2010GL045258, 2010.

27 Mikhailov, E., Vlasenko, S., Martin, S. T., Koop, T., and Poschl, U.: Amorphous and crystalline  
28 aerosol particles interacting with water vapor: conceptual framework and experimental

1 evidence for restructuring, phase transitions and kinetic limitations, *Atmos. Chem. Phys.*, 9,  
2 9491–9522, 2009.

3 Mochida, M. and Kawamura, K.: Hygroscopic properties of levoglucosan and related organic  
4 compounds characteristic to biomass burning aerosol particles, *J. Geophys. Res.*, 109,  
5 D21202, doi: 10.1029/2004JD004962, 2004.

6 Moore, R. H. and Raymond, T. M.: HTDMA analysis of multicomponent dicarboxylic acid  
7 aerosols with comparison to UNIFAC and ZSR, *J. Geophys. Res.*, 113, doi:  
8 10.1029/2007JD008660, 2008.

9 Murphy, D. M., Cziczo, D. J., Froyd, K. D., Hudson, P. K., Matthew, B. M., Middlebrook, A.  
10 M., Peltier, R. E., Sullivan, A., Thomson, D. S., and Weber, R. J.: Single-particle mass  
11 spectrometry of tropospheric aerosol particles, *J. Geophys. Res.*, 111, D23S32, doi:  
12 10.1029/2006JD007340, 2006.

13 Petters, M. D. and Kreidenweis, S. M.: A single parameter representation of hygroscopic  
14 growth and cloud condensation nucleus activity, *Atmos. Chem. Phys.*, 7, 1961-1971, 2007.

15 Pope, F. D., Harper, L., Dennis-Smith, B. J., Griffiths, P. T., Clegg, S. L., and Cox, R. A.:  
16 Laboratory and modeling study of the hygroscopic properties of two model humic acid  
17 aerosol particles, *J. Aerosol Sci.*, 41, 457-467, 2010.

18 Pöhlker, C., Wiedemann, K. T., Sinha, B., Shiraiwa, M., Gunthe, S. S., Smith, M., Su, H.,  
19 Artaxo, P., Chen, Q., Cheng, Y. F., Elbert, W., Gilles, M. K., Kilcoyne, A. L. D., Moffet,  
20 R. C., Weigand, M., Martin, S. T., Pöschl, U., and Andreae, M. O.: Biogenic potassium salt  
21 particles as seeds for secondary organic aerosol in the Amazon, *Science* 337, 1075-1078,  
22 2012.

23 Pöschl, U.: Atmospheric aerosols: composition, transformation, climate and health effects,  
24 *Angew. Chem. Int. Edit.*, 44, 7520–7540, doi:10.1002/anie.200501122, 2005.

25 Prenni, A. J., DeMott, P. J., Kreidenweis, S. M., Sherman, D. E., Russell, L. M., and Ming, Y.:  
26 The effects of low molecular weight dicarboxylic acids on cloud formation, *J. Phys. Chem.*,  
27 105, 11240-11248, 2001.

- 1 Prenni, A. J., DeMott, P. J., and Kreidenweis, S. M.: Water uptake of internally mixed particles  
2 containing ammonium sulfate and dicarboxylic acids, *Atmos. Environ.*, 37, 4243-4251,  
3 2003.
- 4 Raatikainen, T. and Laaksonen, A.: Application of several activity coefficient models to water-  
5 organic-electrolyte aerosols of atmospheric interest, *Atmos. Chem. Phys.*, 5, 2475-2495,  
6 2005.
- 7 Renbaum-Wolff, L., Grayson, J. W., Bateman, A. P., Kuwata, M., Sellier, M., Murray, B. J.,  
8 Shilling, J. E., Martin, S. T., and Bertram, A. K.: Viscosity of  $\alpha$ -pinene secondary organic  
9 material and implications for particle growth and reactivity, *Proc. Natl. Acad. Sci.*, 110,  
10 8014-8019.
- 11 Robinson, C. B., Schill, G. P., and Tolbert, M. A.: Optical growth of highly viscous  
12 organic/sulfate particles, *J. Atmos. Chem.*, 71, 145-156, 2014.
- 13 Saukko, E., Lambe A. T., Massoli, P., Koop, T., Wright, J. P., Croasdale, D. R., Pederna, D. A,  
14 Onasch, T. B., Laaksonen, A., Davidovits, P., Worsnop, D. R., and Virtanen, A.: Humidity-  
15 dependent phase state of SOA particles from biogenic and anthropogenic precursors,  
16 *Atmos. Chem. Phys.*, 12, 7515–7529, 2012.
- 17 Seinfeld, J. H. and Pankow, J. F.: Organic atmospheric particulate matter, *Rev. Phys. Chem.*,  
18 54, 121-140, 2003.
- 19 Seinfeld, J. H. and Pandis S. N.: *Atmospheric Chemistry and Physics*, 2<sup>nd</sup> Edition, John Wiley  
20 & Sons, New York, NY, 2006.
- 21 Shiraiwa, M., Ammann, M., Koop, T., and Pöschl, U.: Gas uptake and chemical aging of  
22 organic aerosol particles, *Proc. Natl. Acad. Sci.*, 108, 11003–11008, 2011.
- 23 Shiraiwa, M., Zuend, A., Bertram, A. K., and Seinfeld, J. H.: Gas-particle partitioning of  
24 atmospheric aerosols: interplay of physical state, non-ideal mixing and morphology, *Phys.*  
25 *Chem. Chem. Phys.*, 15, 1141-11453, 2013.
- 26 Sjogren, S., Gysel, M., Weingartner, E., Baltensperger, U., Cubison, M. J., Coe, H., Zardini, A.  
27 A., Marcolli, C., Krieger, U. K., and Peter T.: Hygroscopic growth and water uptake  
28 kinetics of two-phase aerosol particles consisting of ammonium sulfate, adipic and humic  
29 acid mixtures, *J. Aerosol Sci.*, 38, 157 – 171, 2007.



- 1 Song, M., Marcolli, C., Krieger, U. K., Zuend, A., and Peter, T.: Liquid-liquid phase separation  
2 and morphology of internally mixed dicarboxylic acids/ammonium sulfate/water particles,  
3 *Atmos. Chem. Phys.*, 12, 2691-2712, 2012a.
- 4 Song, M., Marcolli, C., Krieger, U. K., Zuend, A., and Peter, T.: Liquid-liquid phase separation:  
5 Dependence on O:C, organic functionalities, and compositional complexity, *Geophys. Res.*  
6 *Let.*, 39, L19801, doi: 10.1029/2012GL052807, 2012b.
- 7 Song, M., Marcolli, C., Krieger, U. K., Lienhard, D. M., and Peter, T.: Morphologies of mixed  
8 organic/inorganic/aqueous aerosol droplets, *Faraday Discuss.*, 165, 289-316, 2014.
- 9 Sorooshian, A., Hersey, S., Brechtel, F. J., Corless, A., Flagan, R. C., and Seinfeld, J. H.: Rapid,  
10 size-resolved aerosol hygroscopic growth measurements: Differential Aerosol Sizing and  
11 Hygroscopicity Spectrometer Probe (DASH-SP). *Aerosol Sci. Technol.*, 42, 445-464, 2008.
- 12 Svenningsoon, B., Rissler, J., Swietlicki, E., Mircea, M., Bilde, M., Facchini, M. C., Decesari,  
13 S., Fuzzi, S., Zhou, J., Monster, J., and Rosenorn, T.: Hygroscopic growth and critical  
14 supersaturations for mixed aerosol particles of inorganic and organic compounds of  
15 atmospheric relevance, *Atmos. Chem. Phys.*, 6, 1937-1952, 2006.
- 16 Tang, I. N.: Deliquescence properties and particle size change of hygroscopic aerosols, in:  
17 *Generation of Aerosols and Facilities for Exposure Experiments*, K. Willekie, Ed., Ann  
18 Arbor Science Publishers, Ann Arbor, MI, 153-167, 1980.
- 19 Tong, H.-J., Reid, J. P., Bones, D. L., Luo, B. P., and Krieger, U. K.: Measurements of the  
20 timescales for the mass transfer of water in glassy aerosol at low relative humidity and  
21 ambient temperature, *Atmos. Chem. Phys.*, 11, 4739-4754, 2011.
- 22 Vaden, T. D., Imre, D., Beranek, J., Shrivastava, M., and Zelenyuk, A.: Evaporation kinetics  
23 and phase of laboratory and ambient secondary organic aerosol, *Proc. Natl. Acad. Sci.*, 108,  
24 2190 – 2195, 2011.
- 25 Veghte, D. P., Altaf, M. B., and Freedman, M. A.: Size dependence of the structure of organic  
26 aerosol, *J. Am. Chem. Soc.*, 135, 16046-16049.
- 27 Virtanen, A., Joutsensaari, J., Koop, T., Kannosto, J., Yli-Pirila, P., Leskinin, J., Makela, J. M.,  
28 Holopainen, J. K., Poschl, U., Kulmala, M., Worsnop, D. R., and Laaksonen A. An  
29 amorphous solid state of biogenic secondary organic particles. *Nature*, 467, 824–827, 2010.

1 Wise, M. W., Surratt, J. D., Curtis, D. B., Shilling, J. E., and Tolbert, M. A.: Hygroscopic  
2 growth of ammonium sulfate/dicarboxylic acids, *J. Geophys. Res.*, 108, doi:  
3 10.1029/2003JD003775, 2003.

4 Xu, W., Guo, S., Gomez-Hernandez, M., Zambora, M. L., Secret, J., Marrero-Ortiz, W.,  
5 Zhang, A. L., Collins, D. R., and Zhang, R.: Cloud forming potential of oligomers relevant  
6 to secondary organic aerosols, *Geo. Phys. Res. Lett.*, 41,6538–6545, 2014.

7 You, Y., Renbaum-Wolff, L., Carreras-Sospedra, M., Hanna, S. J., Hiranuma, N., Kamal, S.,  
8 Smith, M. L., Zhang, X. L., Weber, R. J., Shilling, J. E., Dabdub, D., Martin, S. T., and  
9 Bertram, A. K.: Images reveal that atmospheric particles can undergo liquid-liquid phase  
10 separations, *Proc. Natl. Acad. Sci.* 109, 13188-13193, 2012.

11 You, Y., Renbaum-Wolff, L., and Bertram, A. K.: Liquid-liquid phase separation in particles  
12 containing organics mixed with ammonium sulfate, ammonium bisulfate, ammonium  
13 nitrate, or sodium chloride, *Atmos. Chem. Phys.*, 13, 11723-11734, 2013.

14 You, Y. and Bertram, A. K.: Effects of molecular weight and temperature on liquid-liquid  
15 separation in particles containing organic species and ammonium sulfate, *Atmos. Chem.*  
16 *Phys.*, 15, 1351-1365, 2015.

17 You, Y., Smith, M. L., Song, M., Martin, S. T., and Bertram, A. K.: Liquid-liquid phase  
18 separation in atmospherically relevant particles consisting of organic species and inorganic  
19 salts, *Int. Rev. Phys. Chem.*, 33, 43-77, 2014.

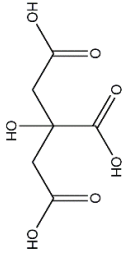
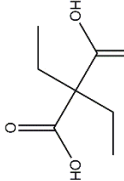
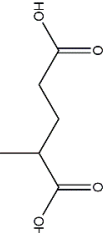
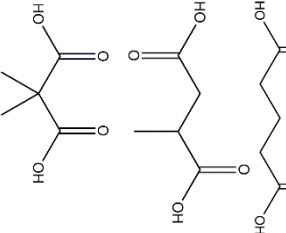
20 Yu, F., Luo, G., and Ma, X.: Regional and global modeling of aerosol optical properties with a  
21 size, composition, and mixing state resolved particle microphysics model, *Atmos. Chem.*  
22 *Phys.*, 12, 5719-5736, 2012.

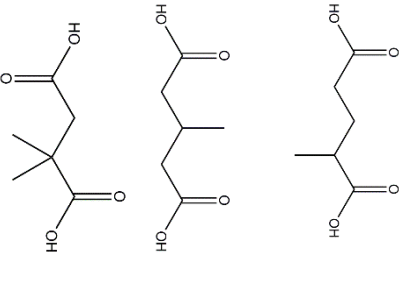
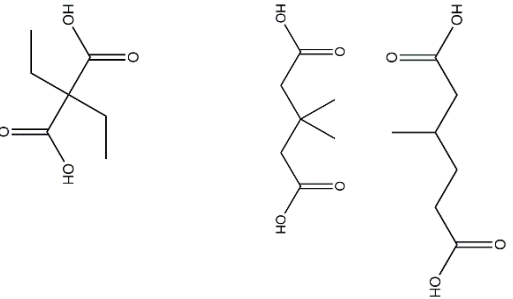
23 Zardini, A. A., Sjogren, S., Marcolli, C., Krieger, U. K., Gysel, M., Weingartner, E.,  
24 Baltensperger, U., and Peter, T.: A combined particle trap/HTDMA hygroscopicity study  
25 of mixed organic/inorganic aerosol particles, *Atmos. Chem. Phys.*, 5589-5601, 2008.

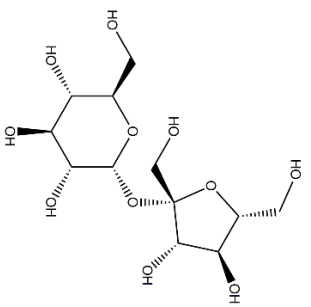
26 Zaveri, R. A., Easter, R. C., Fast, J. D., and Peters, L. K.: Model for Simulating Aerosol  
27 Interactions and Chemistry (MOSAIC), *J. Geophys. Res.*, 113, D13204, doi:  
28 10.1029/2007JD008782, 2008.

- 1 Zaveri, R. A., Easter, R. C., Shilling, J. E., and Seinfeld, J. H.: Modeling kinetic partitioning of  
2 secondary organic aerosol and size distribution dynamics: representing effects of volatility,  
3 phase state, and particle-phase reaction, *Atmos. Chem. Phys.*, 14, 5153-5181, 2014.
- 4 Zhang, Q., Canagaratna, M. R., Jayne, J. T., Worsnop, D. R., and Jimenez, J. L.: Time- and  
5 size-resolved chemical composition of submicron particles in Pittsburgh: Implications for  
6 aerosol sources and processes. *J. Geophys. Res.*, 110, D07S09, doi:  
7 10.1029/2004JD004649, 2005.
- 8 Zobrist, B., Marcolli, C., Pedernera, D. A., and Koop, T. Do atmospheric aerosols form glasses?  
9 *Atmos. Chem. Phys.*, 8, 5221–5244, 2008.
- 10 Zobrist, B., Soonsin, V., Luo, B. P., Kriegerm U. K., Marcolli, C., Peter, T., Koop, T.: Ultra-  
11 slow water diffusion in aqueous sucrose glasses, *Phys. Chem. Chem. Phys.*, 13, 3514-3526,  
12 2011.
- 13 Zuend, A., Marcolli, C., Luo, B. P., and Peter T.: A thermodynamic model of mixed organic-  
14 inorganic aerosols to predict activity coefficients, *Atmos. Chem. Phys.*, 8, 4559–4593,  
15 2008.
- 16 Zuend, A., Marcolli, C., Peter, T., and Seinfeld, J. H.: Computation of liquid-liquid equilibria  
17 and phase stabilities: implications for RH-dependent gas/particle partitioning of organic-  
18 inorganic aerosols, *Atmos. Chem. Phys.*, 10, 7795-7820, 2010.
- 19 Zuend, A., Marcolli, C., Booth, A. M., Lienhard, D. M., Soonsin, V., Krieger, U. K., Topping,  
20 D. O., McFiggans, G., Peter, T., and Seinfeld J. H.: New and extended parameterization of  
21 the thermodynamic model AIOMFAC: calculation of activity coefficients for organic-  
22 inorganic mixtures containing carboxyl, hydroxyl, carbonyl, ether, ester, alkenyl, alkyl, and  
23 aromatic functional groups, *Atmos. Chem. Phys.*, 11, 9155–9206, 2011.
- 24 Zuend, A. and Seinfeld, J. H.: Modeling the gas-particle partitioning of secondary organic  
25 aerosol: the importance of liquid-liquid phase separation. *Atmos. Chem. Phys.*, 12, 3857–  
26 3882, 2012.
- 27 Zuend, A. and Seinfeld, J. H.: A practical method for the calculation of liquid-liquid equilibria  
28 in multicomponent organic-water-electrolyte systems using physiochemical constraints,  
29 *Fluid Phase Equilibria*, 337, 201-213, 2013.

Table 1. Aerosol systems studied

Aerosol System	Organic-Component(s) Structures	Organic-Component(s) Density (kg/m <sup>3</sup> )	Organic:Inorganic Dry Mass Ratio	Previous Experimentally-Determined Phase Behavior	References
Citric Acid + Ammonium Sulfate		1.580	2:1	No LLPS observed	Bertram et al., (2011), You et al. (2013)
Diethylmalonic Acid + Ammonium Sulfate		1.131	2:1	LLPS at RH ≤ 89%	You et al. (2013)
2-Methylglutaric Acid + Ammonium Sulfate		1.169	2:1	LLPS at RH ≤ 75%	You et al. (2013)
C <sub>5</sub> dicarboxylic acids mixture (glutaric, methylsuccinic, dimethylmalonic) + Ammonium Sulfate		1.219	1:1	No LLPS observed	Song et al. (2012a)

<p><math>C_6</math> dicarboxylic acid mixture (2-methylglutaric; 3-methylglutaric, 2,2-dimethylsuccinic) + Ammonium Sulfate</p>		1.169	1:1	<p>Transition from LLPS with partially-engulfed morphology to single liquid phase at RH = 74%</p>	Song et al. (2012a)
<p><math>C_7</math> dicarboxylic acid mixture (3-methyladipic, 3,3-dimethylglutaric, diethylmalonic) + Ammonium Sulfate</p>		1.131	1:1	<p>Transition from LLPS with core-shell morphology to single liquid phase at RH = 89 – 90%</p>	Song et al. (2012a)

Sucrose		1.309	N/A	Glass transition at RH = 24 – 53%, depending on timescale of RH change	Tong et al. (2011), Zobrist et al. (2011)
Sucrose + Ammonium Sulfate			1:1	Unknown	This study
Sucrose + Ammonium Sulfate			2:1	No LLPS observed	You and Bertram (2015)

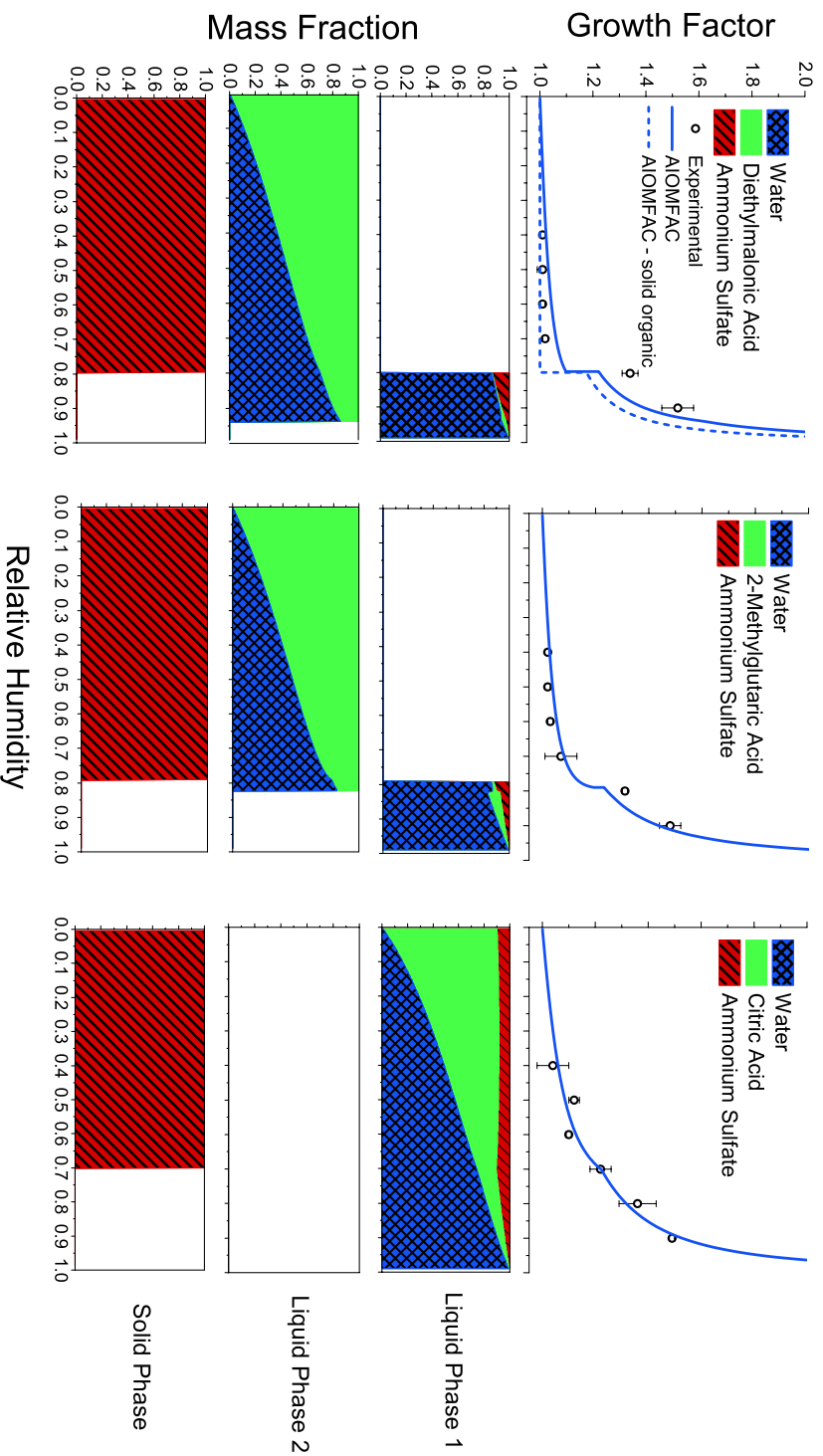


Figure 1. Top panels: Measured and AIOMFAC-predicted hygroscopic diameter growth factors for (a) diethylmalonic acid-ammonium sulfate particles, (b) 2-methylglutaric acid-ammonium sulfate particles, and (c) citric acid-ammonium sulfate particles, with dry organic:inorganic mass ratios of 2:1 for all systems. The black circles indicate the average growth factor measured across ten experiments and error bars indicate the standard deviation of the measured growth factors. Panels below the hygroscopic growth curves indicate the AIOMFAC-predicted composition of each of three possible phases present in the particles (liquid phase 1, liquid phase 2, and a solid phase) as a function of relative humidity. Empty boxes indicate that no second liquid phase is predicted.

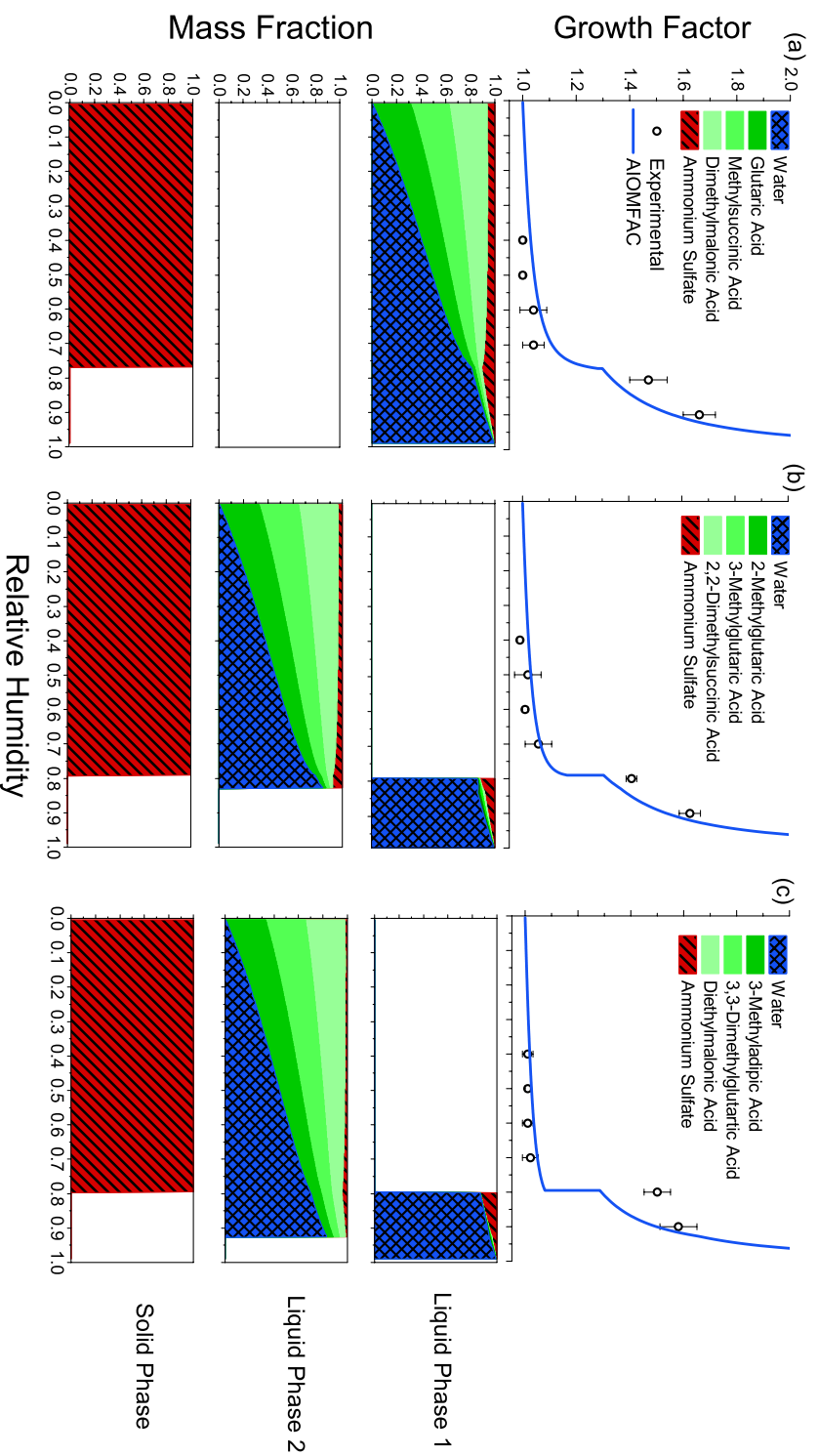


Figure 2. Top panels: Measured and AIOMFAC-predicted hygroscopic diameter growth factors for (a) C<sub>5</sub> dicarboxylic acid mixture-ammonium sulfate particles, (b) C<sub>6</sub> dicarboxylic acid mixture-ammonium sulfate particles, and (c) C<sub>7</sub> dicarboxylic acid mixture-ammonium sulfate particles, with dry organic:inorganic mass ratios of 1:1 for all systems. The black circles indicate the average growth factor measured across ten experiments and error bars indicate the standard deviation of the measured growth factors. Panels below the hygroscopic growth curves indicate the AIOMFAC-predicted composition of each of three possible phases present in the particles (liquid phase 1, liquid phase 2, and a solid phase) as a function of relative humidity. Empty boxes indicate that no second liquid phase is predicted.



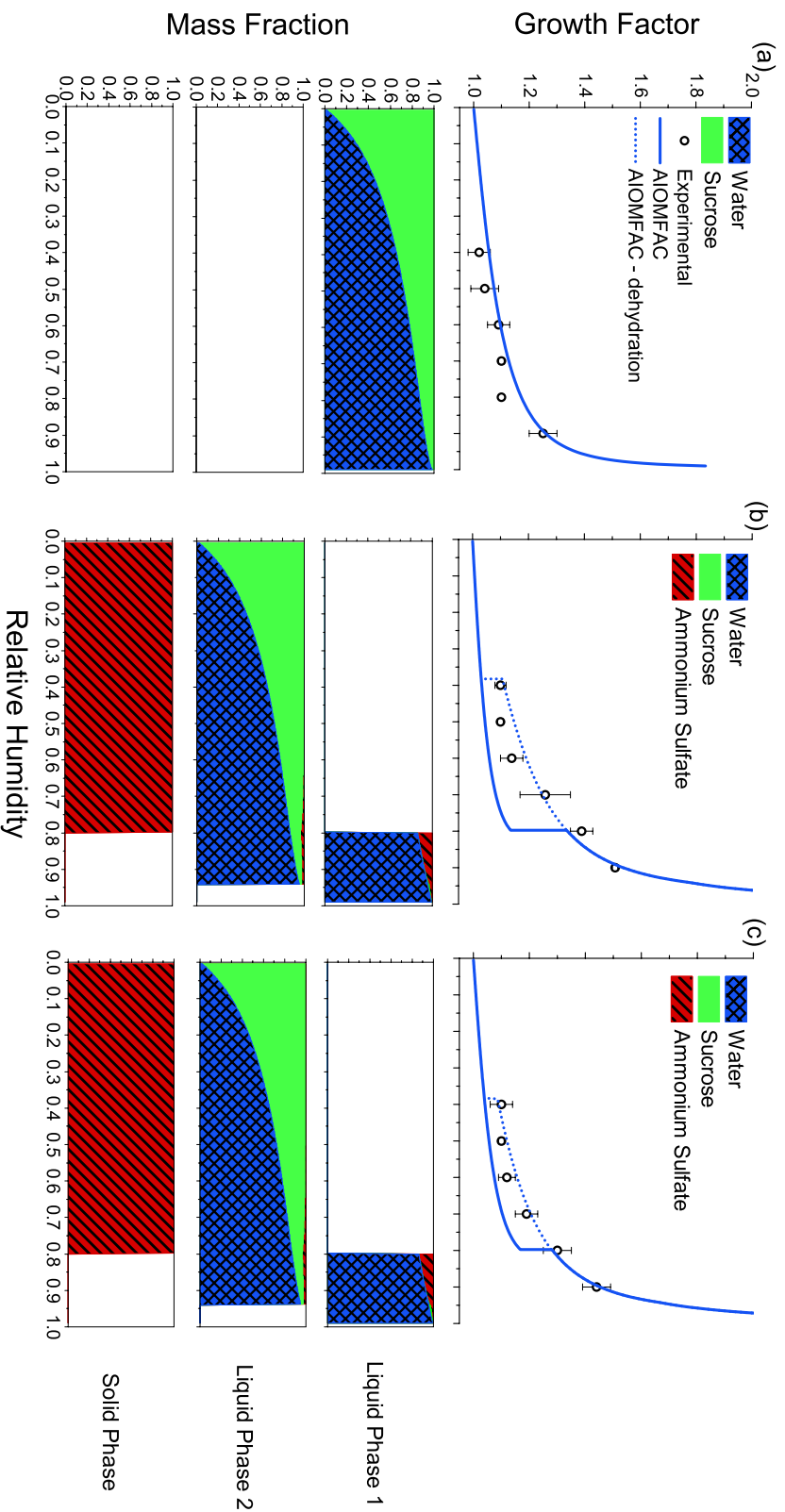


Figure 3. Top panels: Measured and AIOMFAC-predicted hygroscopic growth factors for (a) sucrose particles, (b) mixed sucrose-ammonium sulfate particles with an organic:inorganic ratio of 1:1, and (c) mixed sucrose-ammonium sulfate particles with an organic:inorganic ratio of 2:1. The black circles indicate the average growth factor measured across ten experiments and error bars indicate the standard deviation of the measured growth factors. Solid lines indicate the hydration curve calculated with the AIOMFAC-based equilibrium model, while dashed lines illustrate the dehydration branch in which a supersaturated solution is present

with respect to the dissolved ammonium sulfate. The three panels below the hygroscopic growth curves indicate the AIOMFAC-predicted composition of each of three possible phases present in the particles during the hydration process (liquid phase 1, liquid phase 2, and a solid phase) as a function of relative humidity. Empty boxes indicate that no second liquid phase or no solid phase is predicted.

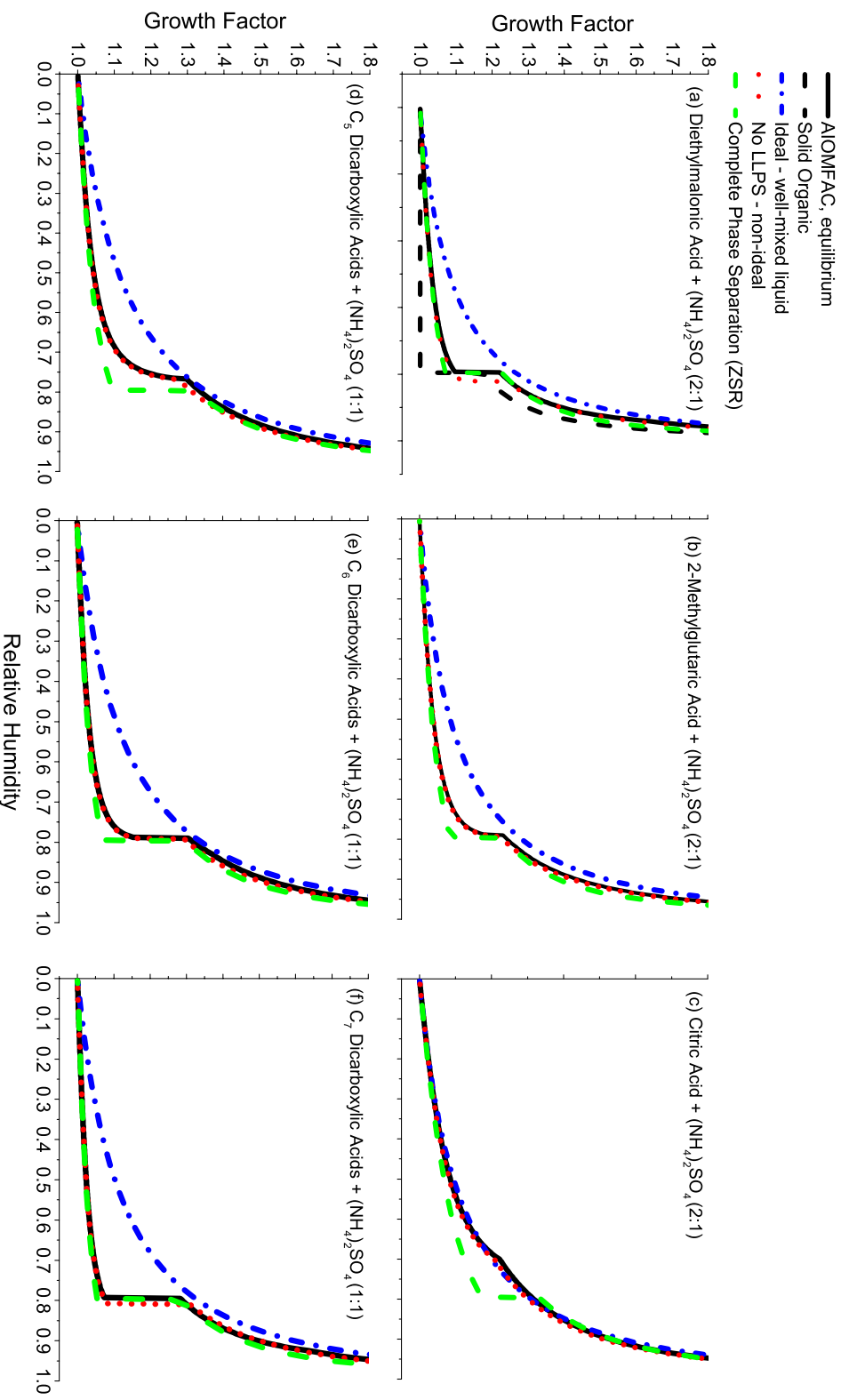


Figure 4. Comparison of simplified thermodynamic assumptions to the full AIOMFAC hygroscopic growth calculations for the multi-component systems for which we expect that observed water-uptake behavior is governed by thermodynamic equilibrium conditions. Organic:inorganic dry mass ratios, which can substantially influence the extent to which non-ideal interactions affect water-uptake, are given in parentheses. The performance of the simplified modeling approaches varies across the systems with variations in phase behavior. Disagreement between the full AIOMFAC-based equilibrium calculations and the simplified models is greatest at low to moderate RH (RH = 20 - 80%).